BIO-INSPIRED TRACTOR-TRAILER DESIGNS FOR AERODYNAMIC DRAG REDUCTION

An Undergraduate Honors Research Thesis

Presented in Partial Fulfillment of the Requirements for

Graduation with Honors Research Distinction in Mechanical Engineering in the

Department of Mechanical and Aerospace Engineering at

The Ohio State University

By

Zachary Zezinka

14 April 2017

Defense Committee:

Dr. Shaurya Prakash, Advisor

Dr. Mohammad Samimy

ABSTRACT

The U.S. economy is dependent on tractor-trailers, which transport $11 trillion in freight annually. Unfortunately, the typical tractor-trailer can travel just 2.5 kilometers per liter (5.8 miles per gallon) of fuel. The poor fuel economy of tractor-trailers can be, in large part, attributed to their poor aerodynamic performance. Outside of engine losses, aerodynamic losses account for the majority of fuel consumption. Since aerodynamic drag is responsible for a large portion of fuel consumption, it is the primary area of focus for improving fuel efficiency of tractor-trailers. Furthermore, current efforts to improve aerodynamic performance of tractor-trailers focus on optimizing tractor design and implementing drag-reducing trailer add-on structures such as skirts and fairings. However, there is currently no practical implementations of improved trailer sidewall design. In fact, trailer sidewall design optimization for drag reduction has been largely overlooked throughout history. One novel path for tractor-trailer drag reduction is to implement trailer sidewall designs that mimic organisms in nature that exhibit low drag. The drag reducing properties of sharkskin have been well researched and allow for superior swimming speed. The unique contours of boxfish also allow for efficient low-drag swimming. Using inspiration from sharkskin and the boxfish, three modified trailer sidewall designs were created. Scale models of the designs, as well as a baseline case, were 3D-printed. The different trailer sidewalls were tested on a scaled tractor-trailer model in a wind tunnel, and along with computational fluid dynamics simulations, it was determined that the bio-inspired designs can reduce the drag coefficient of the baseline design by 12.9 percent. A 12.9 percent reduction in tractor-trailer drag coefficient would produce annual fuel savings of 3 billion liters (780 million gallons) per year across the U.S. tractor-trailer fleet. Although this result is obtained from scaled experiments and numerical simulations, the bio-inspired trailer designs are promising and full-scale experiments are part of the next steps in

proving the feasibility of this technology.

ACKNOWLEDGEMENTS

First and foremost, I would like to thank my advisor Dr. Prakash for his support and mentorship. I would also like to thank Ph.D. student Kaushik Rangharajan for guiding me throughout the duration of this research. The support from everyone at the Microsystems and Nanosystems Laboratory has been instrumental in completing this work. Joe West and Kevin Wolf of the Mechanical and Aerospace Engineering Department also deserve special appreciation for providing technical services required to complete this research. Chris Martin, Tong Lin, and Jason Lamb played necessary roles during the early stages of this project as well.

I would like to thank the College of Engineering and the Department of Energy, through ARPA-E grant no. DE-AR0000282, for financial support. The computing resources provided by the Ohio Supercomputing Center were also extremely helpful in solving the numerical simulations.

Thank you to Dr. Siston and the students enrolled in MECHENG 4999H for the feedback and guidance from the start of the research process. Without the help from all of these individuals and groups, this research would not be possible. Thank you.

TABLE OF CONTENTS

LIST OF FIGURES

LIST OF TABLES

LIST OF EQUATIONS

1.0 INTRODUCTION

1.1 DISCUSSION OF FREIGHT

Tractor-trailers are essential to the United States (U.S.) economy. The annual value of freight transported in the U.S. in 2013 was $18 trillion[1] [1]. Of the $18 trillion[1], $11 trillion[1] or 64% was transported by the trucking industry (see Fig. 1) [1]. The annual distance traveled by the trucking industry on U.S. highways in 2013 was 443 billion kilometers (275 billion miles) [1]. Of the 443 billion kilometers, 271 billion kilometers (168 billion miles) or 61% was traveled by tractor-trailers [1]. Tractor-trailers are the primary vehicle type in the trucking industry, which is a pillar of the U.S. economy.

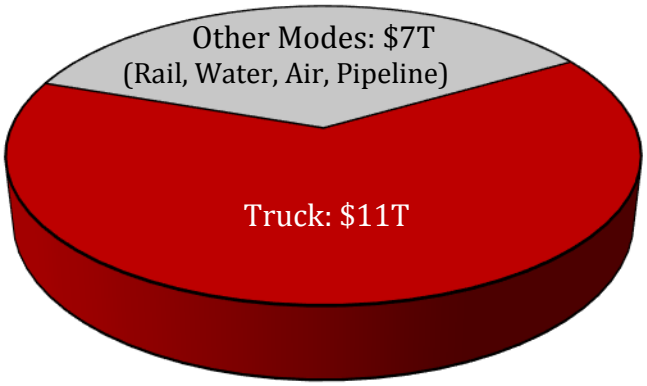

Figure 1: Value of U.S. Shipments by Transportation Mode [1]

The widespread use of tractor-trailers—although essential to the U.S. economy—has consequences. In traveling 271 billion kilometers, tractor-trailers consumed 109 billion liters (29 billion gallons) of fuel, which is 17% of the total U.S. highway fuel consumption [1]. The fact that tractor-trailers consumed 17% of the total U.S. highway fuel consumption is an especially alarming fact when considering tractor-trailers are less than 1% of the total vehicle

[1] 2007 U.S. Dollars

population on U.S. highways (see Fig. 2) [1].

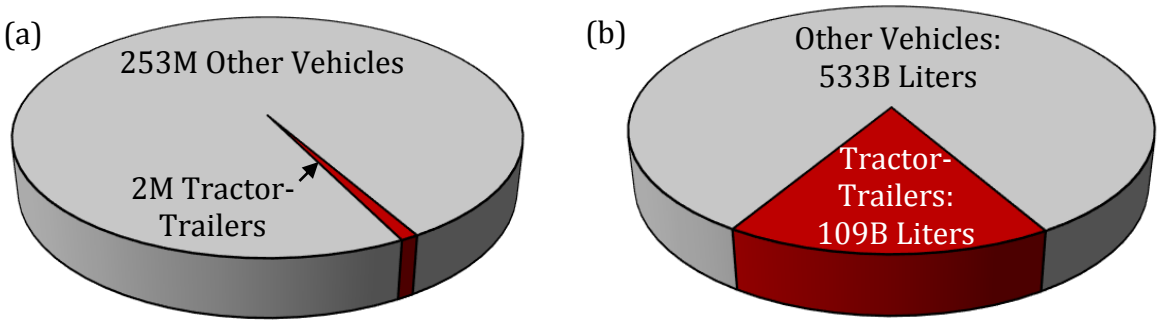

Figure 2: U.S. Highway (a) Vehicle Population (b) Fuel Consumption [1]

The high fuel consumption by tractor-trailers can be partially attributed to their poor fuel economy. On average, tractor-trailers travel just 2.5 kilometers per liter (5.8 miles per gallon) of fuel on U.S. highways [1]. For comparison, the similarly diesel powered 2017 BMW 328d has a fuel economy of 18 kilometers per liter (43 miles per gallon) on U.S. highways (See Fig. 3) [2].

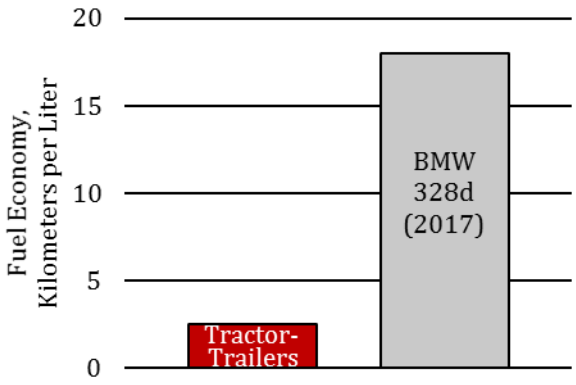

Figure 3: Highway Fuel Economy Comparison [1, 2]

On a per mile basis, the comparatively lower fuel economy of tractor-trailers yields higher fuel costs and higher greenhouse gas emissions as a result of higher fuel consumption. The preceding issues are compounded when considering the uncertainty of fuel prices and

concerns surrounding greenhouse gas emissions [3-7].

In order to abate the aforementioned issues so that tractor-trailers can continue to play an essential role in U.S. commerce, the fuel economy of tractor-trailers must be improved. To improve the fuel economy of tractor-trailers, the focus of this thesis is on improving the aerodynamic performance of tractor-trailers. Outside of engine losses, aerodynamic losses account for the largest fraction of fuel consumption for tractor-trailers [8]. For a tractor-trailer traveling with a full load at a typical highway speed such as 29 meters per second (65 miles per hour), 21% of fuel is consumed in overcoming the resistance caused by aerodynamic drag (see Fig. 4) [8]. This means that for every one percent reduction in aerodynamic drag, fuel economy is increased by roughly 0.22% and fuel consumption is decreases by roughly 0.21%.

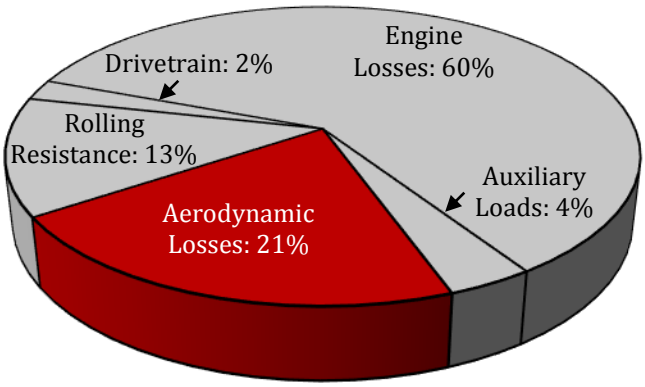

Figure 4: Tractor-trailer Fuel Consumption [8]

Aerodynamic drag is the sum of pressure drag and skin friction drag [9]. For a tractor-trailer traveling at a typical highway speed such as 25 meters per second (56 miles per hour), pressure drag accounts for over 90% of the total aerodynamic drag [10]. Pressure drag is dominant due in large part to stagnated flow at the leading edge of the tractor and flow separation at the trailing edge of the trailer [11]. The general flow patterns described

previously produce a pressure drop from the front to the rear of the tractor-trailer, which gives rise to pressure drag [11]. If the flow separation and pressure drop are reduced, the pressure drag and thus total aerodynamic drag acting on the tractor-trailer will also be reduced.

Academia and industry have been studying and implementing devices and design modifications aimed at reducing drag on tractor-trailers [12]. The first generation of drag reducing efforts focused on altering tractor design with the implementation of features such as cab shaping and rounding, roof fairings, side extenders, and chassis skirts (see Fig. 5) [12]. The preceding efforts were capable of reducing aerodynamic drag by 15 – 31% [12].

Figure 5: Tractor-Trailer (a) without First Generation Features [12] (b-d) with First Generation Features [13]

Following the first generation efforts, which focused on the tractor, a second generation of drag reduction efforts began and focused on trailer add-on devices [12]. The second generation of features included gap seals, trailer skirts, and base flaps, which reduced aerodynamic drag by an additional 3 – 15% (see Fig. 6) [12].

Figure 6: Second Generation Drag Reduction Devices [14]

Today, the next generation of innovations are being developed thanks to the SuperTruck initiative started by the U.S. Department of Energy [15]. Four industry teams participated in the first SuperTruck initiative and all surpassed the primary objective of increasing freight efficiency by 50% (see Fig. 7) [16-19].

Figure 7: SuperTrucks by (a) Cummins-Peterbilt [16] (b) Daimler [15] (c) Navistar [20] (d) Volvo [21]

Despite all of the innovation that has occurred, there has been limited exploration into modifying the design of the trailer sidewalls. Although the trailer was an area of focus for the second generation of drag reduction techniques, the design of trailer sidewalls remained the same [12]. Even the most advanced tractor-trailer designs found in the SuperTruck initiative feature trailers with planar sidewalls [15, 16, 20, 21]. A review of U.S. patents, listed in Appendix A: Patent Review, also showed limited exploration into the modification of trailer sidewalls for drag reduction on tractor-trailers. It is because of this lack of exploration that the focus of this thesis is on developing trailer sidewall designs capable of improving the aerodynamic performance of tractor-trailers.

1.2 DISCUSSION OF BIO-INSPIRED DESIGN

To gain insight on how to design modified trailer sidewalls for tractor-trailer drag

reduction, nature was used as a source of inspiration. Nature is a useful source of design inspiration because—through evolution—nature has developed highly optimized and high performance systems [22]. Aquatic animals are of special interest because they have developed morphologies and features capable of reducing hydrodynamic drag, which allows for efficient movement in water [22]. For instance, marine boxfishes (Teleostei: Ostraciidae)—despite their blunt bodies—are able to swim up to six body lengths per second because of their rigid keeled exteriors [22, 23]. The shape of the boxfish was used as inspiration for a bionic concept car built by Mercedes Benz that showed low aerodynamic drag and high fuel economy [22].

In addition to the boxfish, the drag reducing properties of sharkskin has also been heavily investigated [22]. Sharks are covered in dermal denticles, which control boundary-layer separation and reduce eddy formation [22]. This allows sharks like the shortfin mako (Isurus oxyrhynchus) to travel at speeds reaching 9.8 meters per second (22 miles per hour) [24]. It is hypothesized that sharkskin will also reduce aerodynamic drag when applied to a tractor-trailer based on Reynolds number similarity.

$$Re = \rho v L / \mu$$ Equation 1: Reynolds Number

Re = Reynolds number

ρ = Density of fluid

v = Velocity of fluid with respect to body

L = Length of body measured in direction of fluid velocity

μ = Dynamic viscosity of fluid

Table 1: Properties for Shortfin Mako and Tractor-trailer Flow

	Shortfin Mako (Fluid: Seawater)	Tractor-trailer (Fluid: Air)
ρ (kg/m^3)	1030 [25]	1.23 [25]
v (m/s)	9.83 [24]	29.1 [8]
L (m)	3.28 [26]	22.5 [10]
μ (Pa-s)	1.20×10^{-3} [25]	1.79×10^{-5} [25]

Using the preceding equation and table of values, the Reynolds number for both the shortfin mako and tractor-trailer is $O(10)^7$ which indicates similar flow characteristics.

The success of the boxfish inspired concept car by Mercedes Benz and the Reynolds number similarity of the shortfin mako and tractor-trailer motivated the conception of three alternative trailer sidewall designs. The first design is inspired by the morphology of the boxfish, the second design is inspired by the skin of sharks, and the third design is a hierarchical combination of the first and second designs.

1.3 OVERVIEW OF THESIS

The proposed alternative trailer sidewall designs are described in greater detail in Chapter 2.0 Tractor-Trailer Design. The design of the modular tractor-trailer which enables the testing of the alternative trailer sidewall designs—as well as a baseline or control trailer sidewall design—is also discussed in Chapter 2.0 Tractor-Trailer Design. Chapter 3.0 Methodology outlines the procedure for which wind tunnel experiments were carried out to evaluate the performance of the trailer sidewall designs. The methods employed in the accompanying numerical simulations are also discussed in Chapter 3.0 Methodology. Chapter

4.0 Results and Discussion reviews the performance of the alternative trailer sidewall designs against the baseline. The fifth and final chapter of this thesis, Conclusion, provides important takeaways from this research as well as future work and a closing summary.

2.0 TRACTOR-TRAILER DESIGN

A 1:40 scale modular tractor-trailer was created in SolidWorks to enable the evaluation of the alternative trailer sidewall designs in wind tunnel experiments (see Fig. 8).

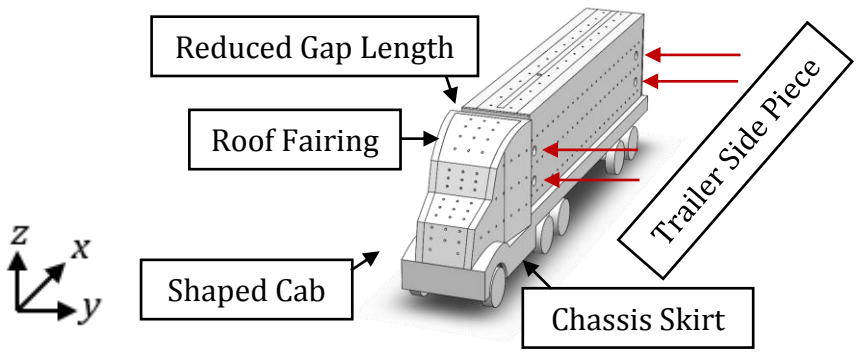

Figure 8: Tractor-trailer Model without Trailer Sidewall Pieces Attached

The model features four peg holes on both sides of the trailer so that the four trailer sidewall pieces—the baseline and three alternatives—can be swapped in and out for testing. The model is also covered with 294 pressure taps of 1.59 millimeter (1/16 inch) diameter to enable the measurement of the pressure distribution around the model. The top of the model also features a threaded hole so that it can be suspended in the wind tunnel from the test stand, which measures the drag force acting on the model. The model also incorporates the first generation drag reduction features currently used in the trucking industry: cab shaping, roof fairing, reduced gap length (represents side extenders), and chassis skirt [12]. Table 2 highlights the important dimensions of the model.

Table 2: Tractor-Trailer Model General Dimensions (1:40 Scale)

	Metric Units, centimeters	English Units, inches
Overall Length	38.4	15.1
Trailer Length	28.4	11.2
Overall Height	11.4	4.5
Tractor Width	6.1	2.4

The tractor-trailer model was fabricated using fused deposition modeling. A Fortus 400mc 3D printer manufactured by Stratasys was used to print the model out of polycarbonate.

2.1 BASELINE DESIGN

The baseline trailer design is simply a planar sidewall, which represents the state of the art in the trucking industry (see Fig. 9). With this trailer sidewall installed on the tractor-trailer model, the trailer width is 6.1 centimeters (2.4 inches) and the projected area of the model is 65.2 square centimeters (10.1 square inches).

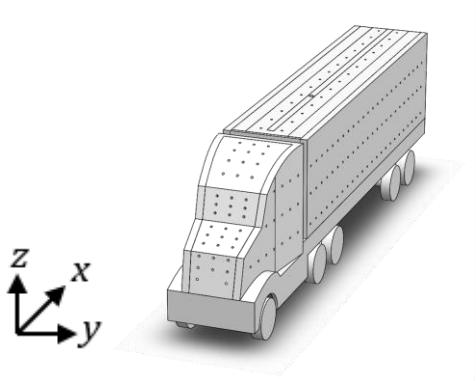

Figure 9: Tractor-trailer Model with Baseline Trailer Sidewall Design

2.2 BOXFISH INSPIRED DESIGN

The boxfish inspired trailer sidewall design is a plate featuring a contoured profile of constant radius (see Fig. 10). The radius of the contour is 199.4 centimeters (78.5 inches) and increases the width of the trailer by 0.3 centimeters (0.1 inches) on each side of the trailer in comparison to the baseline. With this trailer sidewall installed on the tractor-trailer model, the trailer width is 6.6 cm (2.6 inches) and the projected area of the model is 68.7 square centimeters (10.7 square inches).

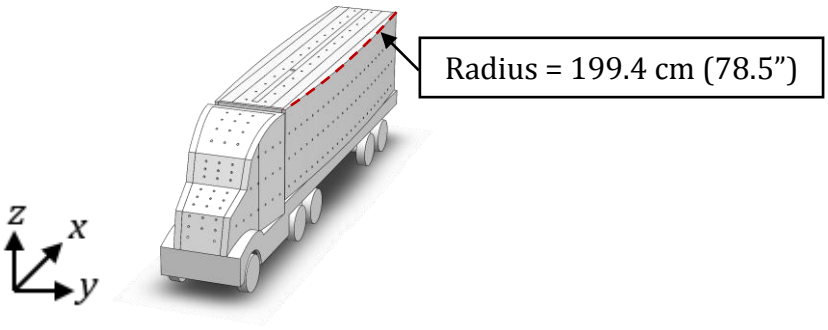

Figure 10: Tractor-trailer Model with Boxfish Inspired Trailer Sidewall Design

2.3 SHARK INSPIRED DESIGN

The shark inspired trailer sidewall design is a flat plate with an array of features inspired by the dermal denticles found on sharkskin (see Fig. 11). There are 25 staggered rows of features in the vertical (z) direction with 0.25 millimeter (0.01 inch) spacing between the rows. The odd numbered rows have 27 features in the direction of motion (x) and the even numbered rows have 26 features in the direction of motion (x). The features are 2.5 millimeters (0.1 inches) in the vertical direction (z), 1.0 centimeters (0.4 inches) in the direction of motion (x), and 2.5 millimeters (0.1 inches) in the third direction (y). With this trailer sidewall installed on the tractor-trailer model, the trailer width is 6.4 centimeters (2.5

inches) and the projected area of the model is 65.7 square centimeters (10.3 square inches).

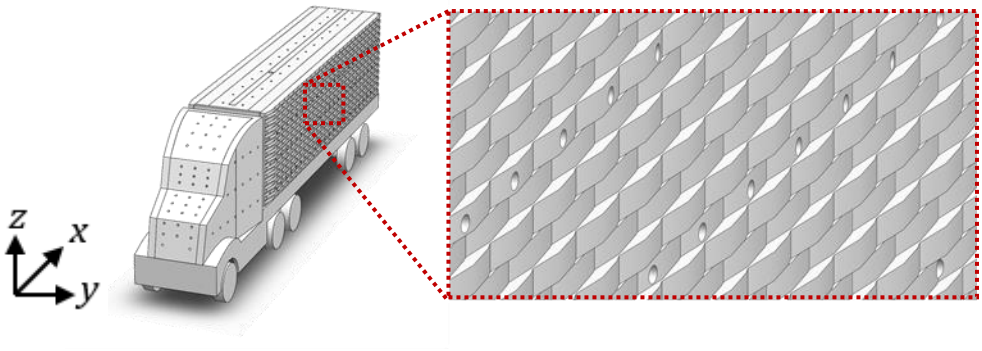

Figure 11: Tractor-trailer Model with Shark Inspired Trailer Sidewall Design

2.4 BOXFISH + SHARK INSPIRED DESIGN

This hierarchical trailer sidewall design combines the boxfish and shark inspired designs. Features inspired by the dermal denticles of sharkskin are placed in an array, which conforms to a contoured profile of constant radius (see Fig. 12). The radius of the contour is 199.4 centimeters (78.5 inches) like in the boxfish inspired trailer side design. The array of features inspired by sharkskin is 25 staggered rows in the vertical direction (z) with 0.25 millimeter (0.01 inch) spacing. Each row contains 15 features in the direction of motion (x). The features are 2.5 millimeters (0.1 inches) in the vertical direction (z), 1.8 centimeters (0.7 inches) in the direction of motion (x), and 2.5 millimeters (0.1 inches) in the third direction (y). With this trailer sidewall installed on the tractor-trailer model, the trailer width is 7.1 centimeters (2.8 inches) and the projected area of the model is 71.5 square centimeters (11.1 square inches).

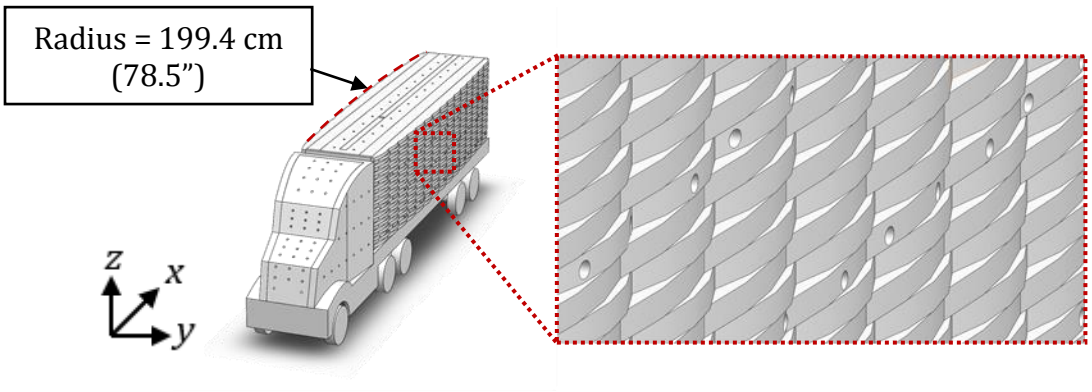

Figure 12: Tractor-trailer Model with Boxfish + Shark Inspired Trailer Sidewall Design

3.0 METHODODOLOGY

3.1 WIND TUNNEL EXPERIMENTAL METHOD

To evaluate the efficacy of the proposed alternative trailer sidewall designs, they—along with the baseline—were tested in a wind tunnel where drag and pressure measurements were recorded. The wind tunnel was constructed in the basement of Scott Laboratory on the Ohio State University campus in Columbus, OH. The wind tunnel was made up of three main sections: the contraction section, the diffuser section, and the test section (see Fig. 13).

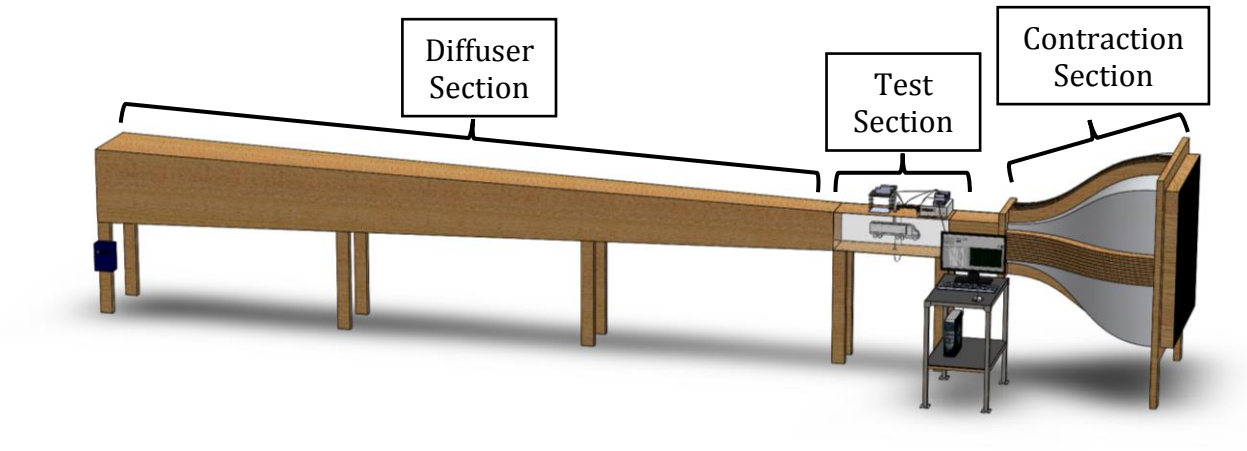

Figure 13: Wind Tunnel Schematic

The contraction section is where the air enters the wind tunnel. The air enters through a 1.2 meter (48 inch) by 1.2 meter inlet and is aligned using a honeycomb screen. Over the 1.2 meter (48 inch) length of the contraction section, the cross section is reduced to 30 centimeters (12 inches) by 30 centimeters. The decrease in cross sectional area is achieved using contraction curves defined by a fifth order polynomial that allows for smooth flow profiles [27]. As a result of the reduced cross sectional area, the airflow accelerates to the test section air speed.

The diffuser section is where the air exits the wind tunnel. The diffuser section comprises the majority of the length of the wind tunnel. The cross sectional area of the diffuser section increases gradually to meet the fan/motor assembly, which pulls the air through the wind tunnel. The fan/motor assembly is controlled by a variable power box, which allows for different air speeds to be used in the test section. In order to run experiments at known test section air speeds, the wind tunnel was calibrated by varying the readout on the fan/motor variable power box and measuring the air speed in the test section with an Ambient Weather WM-2 Handheld Weather Meter (see Fig. 14).

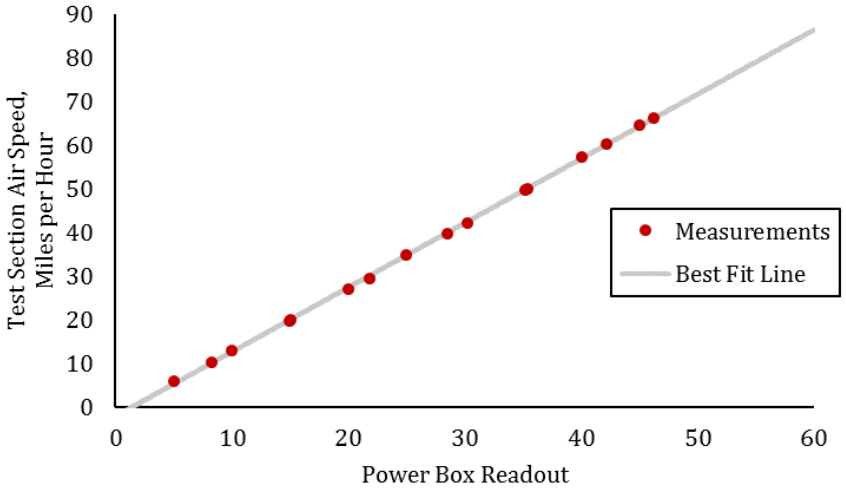

Figure 14: Wind Tunnel Air Speed Calibration

In between the contraction and diffuser sections is the test section (see Fig. 15). The test section is where the tractor-trailer model is mounted and where all of the data acquisition equipment is located. Drag and pressure measurements can be made on the tractor-trailer model in the test section.

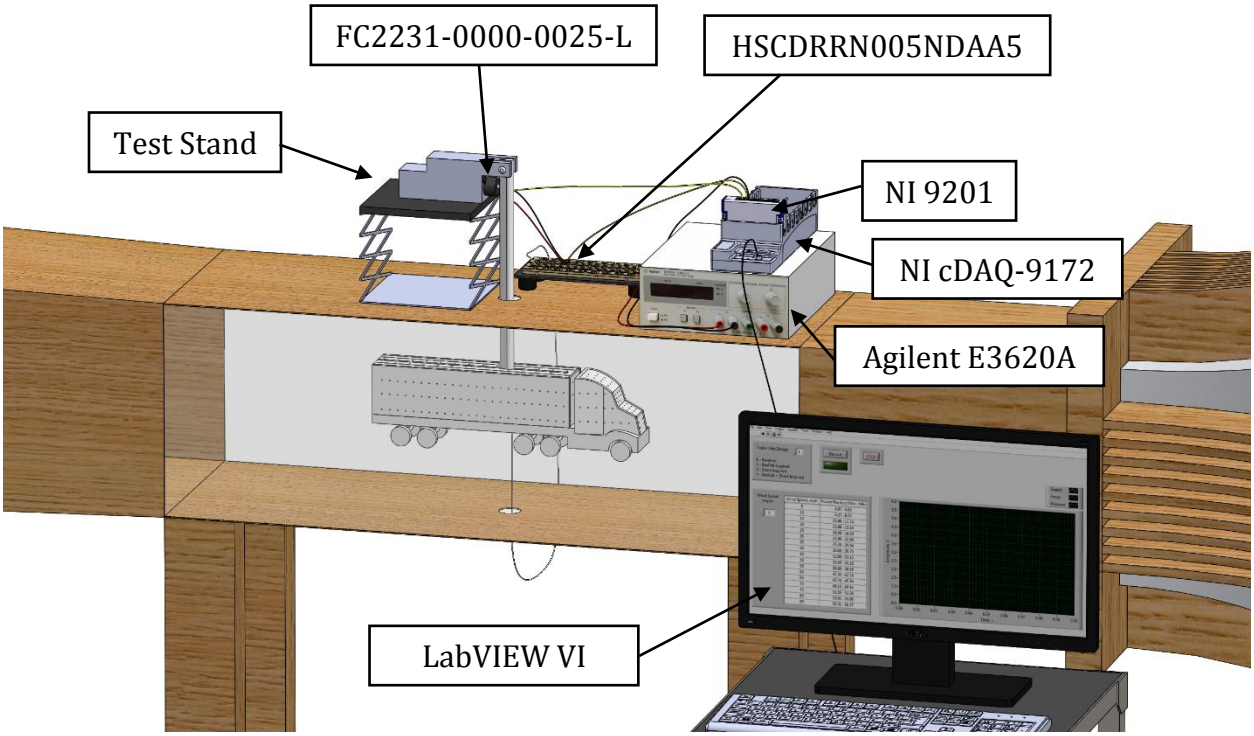

Figure 15: Test Section Schematic

To determine the drag force acting on the tractor-trailer model in the wind tunnel, the test stand and FC2231-0000-0025-L compression load cell from TE Connectivity was calibrated. The proceeding figure plots the calibration measurements over the design stage calibration curve derived from the system geometry and the values found in the load cell data sheet [28]. The coefficient of determination or R^2 value was greater than 0.99 for the calibration measurements and design stage calibration curve so the expression for the design stage calibration curve was used in the data processing programming found in

Appendix B: Drag Data Processing with Matlab.

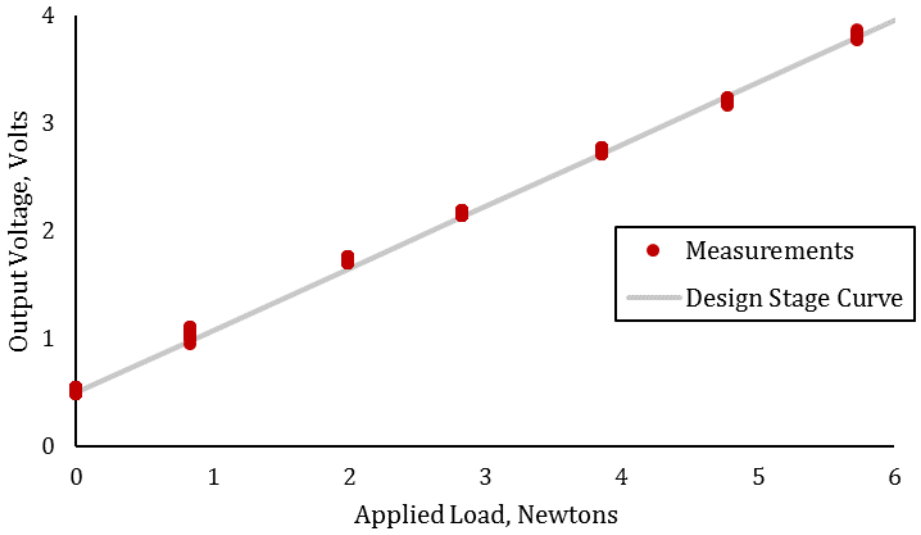

Figure 16: Test Stand/Load Cell Drag Force Calibration

Once load cell output voltage data was converted to drag force data using the calibration curve above, it was then non-dimensionalized and reported as the drag coefficient using the following equation.

$$C_D = \frac{2F_D}{\rho v^2 A}$$ Equation 2: Drag Coefficient

C_D = Drag coefficient

F_D = Drag force

ρ = Density of air

v = Velocity of air with respect to tractor-trailer model

A = Projected area of tractor-trailer model

Pressure was measured around the body of the tractor-trailer model in the wind tunnel using a HSCDRRN005NDAA5 differential pressure sensor from Honeywell. The differential pressure sensor was open to the laboratory atmosphere—away from the wind tunnel inlet and outlet—at one terminal and connected to one of 294 pressure taps at the opposite terminal via tubing. Pressure taps of 1.59 millimeter (1/16 inch) diameter were distributed around the tractor-trailer model to obtain pressure distributions. The transfer function provided by the manufacturer in the data sheet was used in the data processing programming [29].

Data was collected using National Instruments hardware (NI cDAQ-9172 and NI 9201) and software (LabVIEW). A LabVIEW Virtual Instrument File was written which allowed sensor output signals to be monitored and recorded. Data was recorded at 10 Hz for 100 seconds for measurements at a given test condition. Data was processed and analyzed in Microsoft Excel and MATLAB.

3.2 NUMERICAL METHODS

Numerical simulations of the tractor-trailer model were performed by Ph.D. student Kaushik Rangharajan to validate experimental results and test the feasibility of the designs at full scale. COMSOL Multiphysics was used for the simulations along with computing resources from the Ohio Supercomputer Center. A Reynolds averaged Navier-Stokes solver utilizing the 2-equation k-ε model of turbulence was used for the simulations. This method was validated using the Ahmed body benchmark. The drag coefficient obtained in the validation simulation was within 1% of previously reported values [30].

4.0 RESULTS AND DISCUSSION

4.1 WIND TUNNEL EXPERIMENTS

The proceeding figure illustrates the drag results of the wind tunnel experiments.

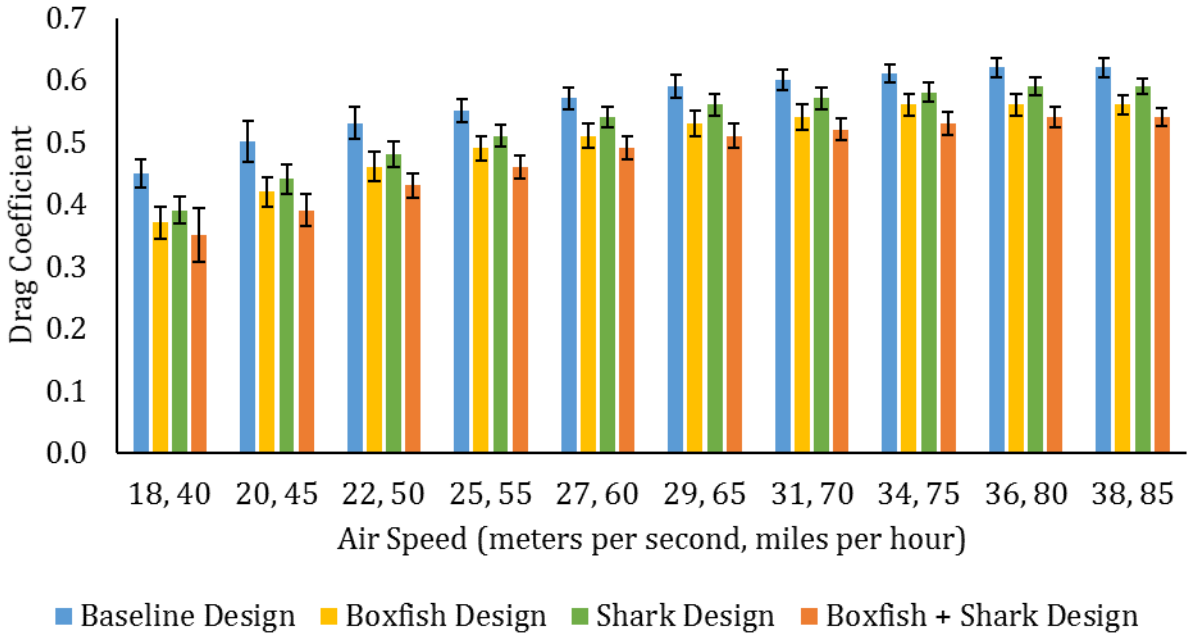

Figure 17: Wind Tunnel Drag Results

At all tested air speeds, the drag coefficient for each of the three alternative trailer sidewall designs were lower than that of the baseline. When compared to the baseline case, the shark inspired design reduced the drag coefficient and to a greater extent so did the boxfish inspired design. The hierarchical boxfish + shark inspired design reduced the drag coefficient by an even larger amount. To ensure the drag reduction results were statistically significant from the baseline case, 2-sample t-tests were performed at a significance level of 0.01. All drag reduction results were determined to be statistically significant from the baseline.

At the 38 meters per second test condition, the drag coefficient for the baseline design was 0.62. The boxfish inspired design was able to reduce the drag coefficient to 0.56, which is

9.7% lower than the baseline. The shark inspired design was able to reduce the drag coefficient to 0.59, which is 4.8% lower than the baseline. The boxfish + shark inspired design was able to reduce the drag coefficient to 0.54, which is 12.9% lower than the baseline.

Evidence of reduced drag was also observed in the pressure measurement data. The maximum pressure drop from the front of the tractor-trailer model to the rear was lower for the three alternative designs in comparison to the baseline design (see Table 3).

Table 3: Tractor-Trailer Pressure Drop from Front to Back at 38 m/s

	Pressure Drop (Non-Dimensionalized)
Baseline Design	0.43
Boxfish Inspired Design	0.42
Shark Inspired Design	0.42
Boxfish + Shark Inspired Design	0.40

The boxfish + shark inspired design showed the lowest pressure drop from the front of the tractor to the back of the trailer, which is in agreement with the fact that this design also had the lowest measured drag coefficient.

4.2 NUMERICAL SIMULATIONS

Numerical simulations were performed to better understand the results obtained in the wind tunnel. The proceeding figure illustrates the region behind the tractor-trailer model for the baseline and boxfish inspired design.

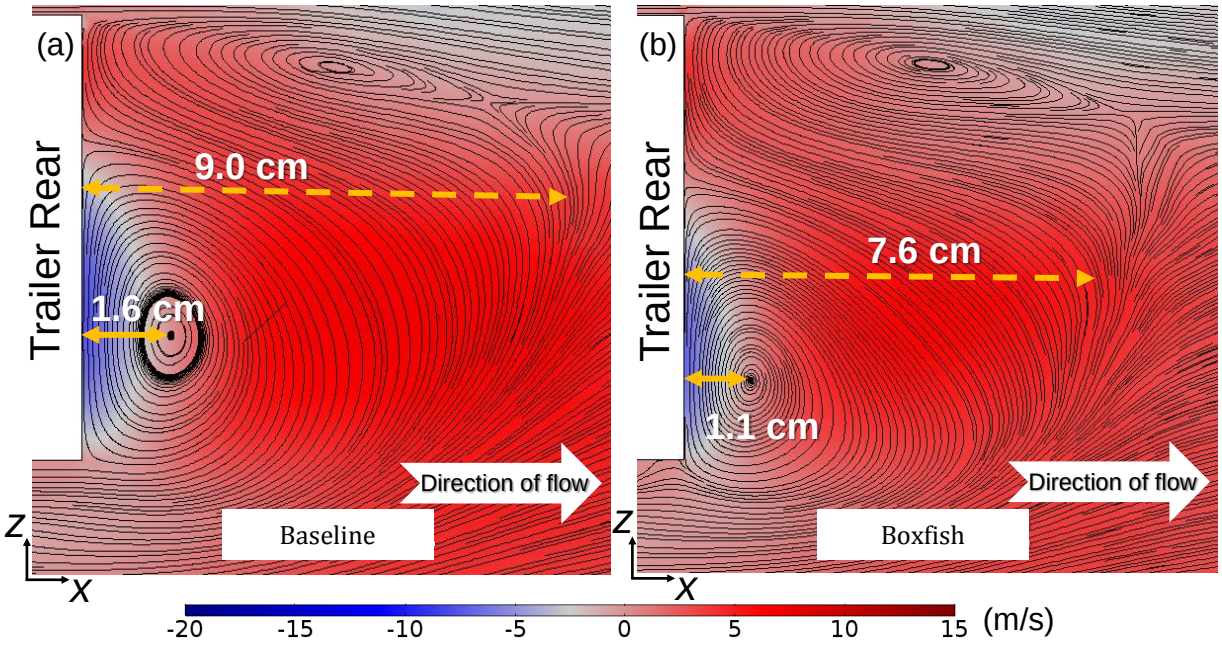

Figure 18: Region Behind (a) Baseline and (b) Boxfish Inspired Design (1:40 scale at 38 m/s)

Based on the results of the simulation, the boxfish inspired trailer sidewall design was effective at reducing the recirculation length. As a result of the reduced recirculation length, the pressure incident on the back of the trailer was greater for the boxfish design in comparison to the baseline as shown in the proceeding figure.

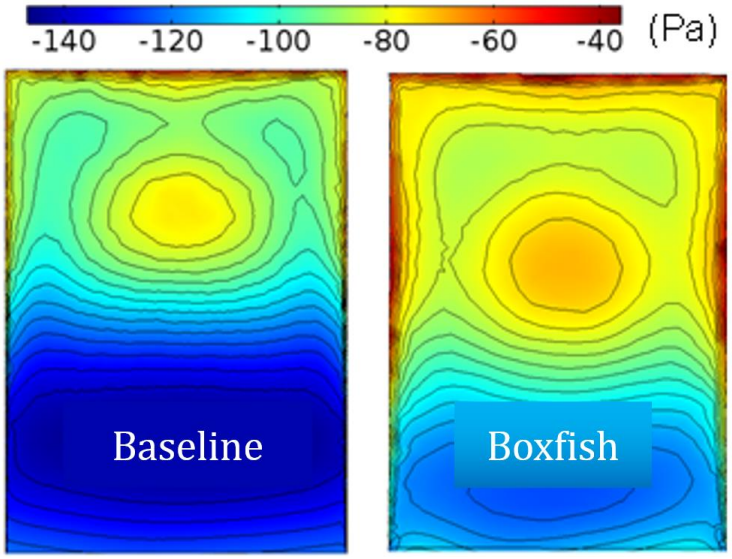

Figure 19: Pressure on Back of Trailer for Baseline and Boxfish Design (1:40 Scale at 38 m/s)

The increased pressure on the back of the trailer for the boxfish design is in agreement with the pressure measurements obtained in the wind tunnel experiment as well as the drag coefficient results.

The proceeding figure illustrates the numerically estimated boundary layer for the baseline and shark inspired design.

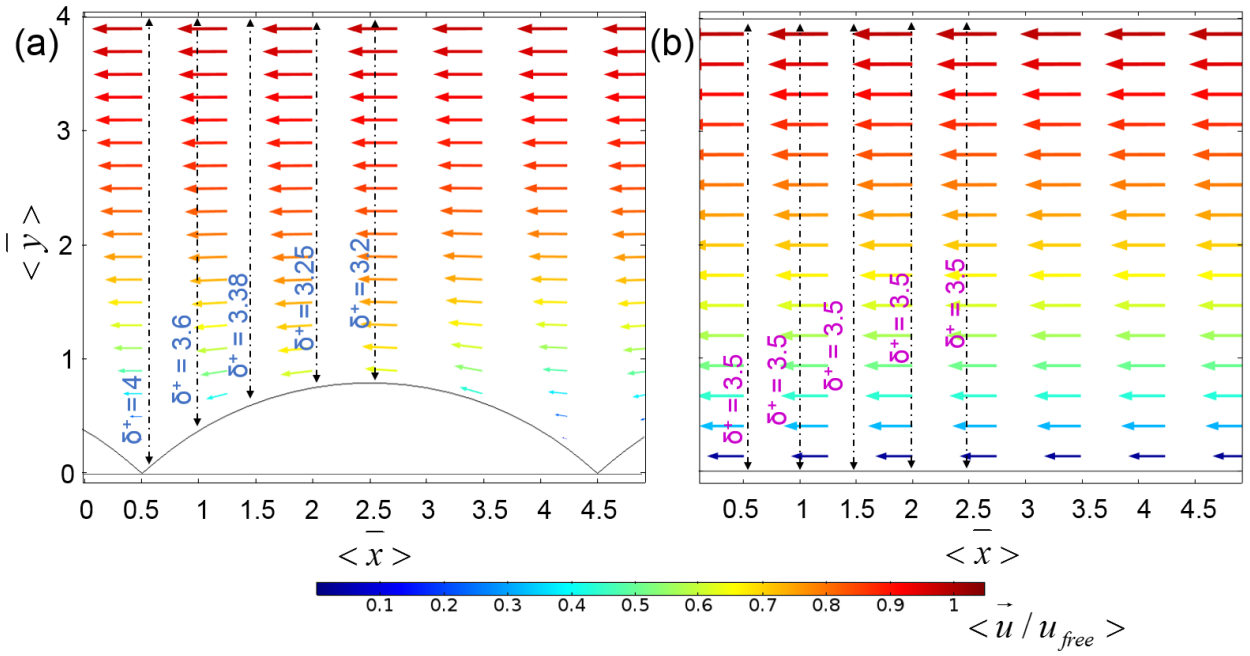

Figure 20: Boundary Layer Profile (a) Shark Design (b) Baseline (1:40 scale, 38 m/s)

According to the numerical simulations, the shark inspired trailer sidewall design was effective at reducing the boundary layer thickness, which translates to less severe flow separation at the rear of the tractor-trailer model. Less severe flow separation at the rear of the tractor-trailer model is associated with lower aerodynamic drag and so these results are in agreement with the drag coefficient results of the previous section, which stated that the shark inspired design experienced reduced drag in comparison to the baseline.

The boxfish + shark inspired trailer sidewall design experienced the least drag because

it utilized the drag reducing mechanisms present in both the boxfish inspired and shark inspired designs.

4.3 WIND TUNNEL EXPERIMENTS AND NUMERICAL SIMULATIONS COMPARISON

The proceeding figure provides a side-by-side comparison of the pressure distribution around the tractor-trailer model obtained from the wind tunnel experiments and from the numerical simulations for the baseline case at the 38 meters per second (85 miles per hour) air speed condition.

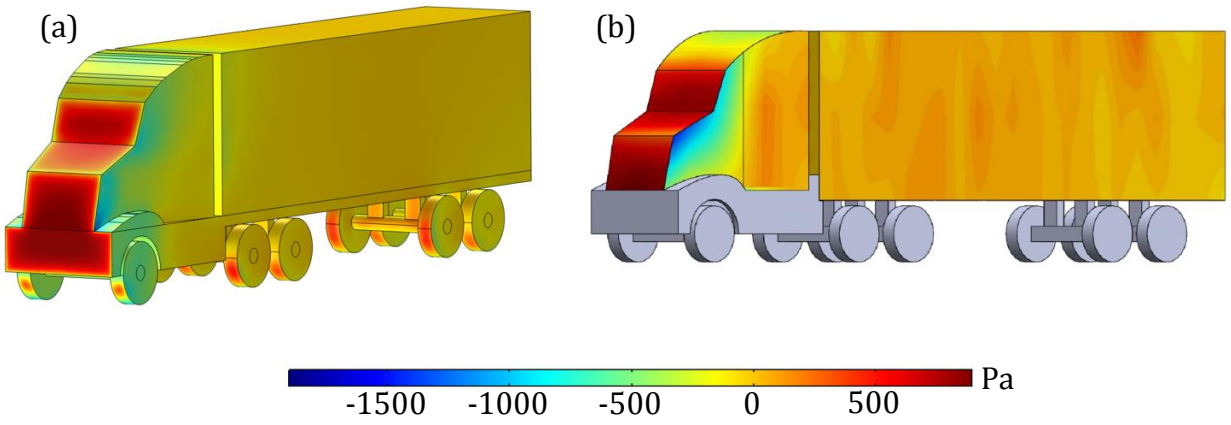

Figure 21: Baseline Pressure Distribution (a) Simulation (b) Wind Tunnel (1:40 Scale, 38 m/s)

The pressure distributions above are in good agreement with each other as well as with the expectations based on theory. In both pressure distributions, the highest pressure occurs at the front of the tractor where flow is expected to stagnate. Low pressure regions are also observed on the side of the tractor where flow separation is expected to occur.

Full-scale tractor-trailer simulations were also completed. Drag coefficient results of full-scale simulations, along with results from the wind tunnel experiments and 1:40 scale simulations are provided in the proceeding figure.

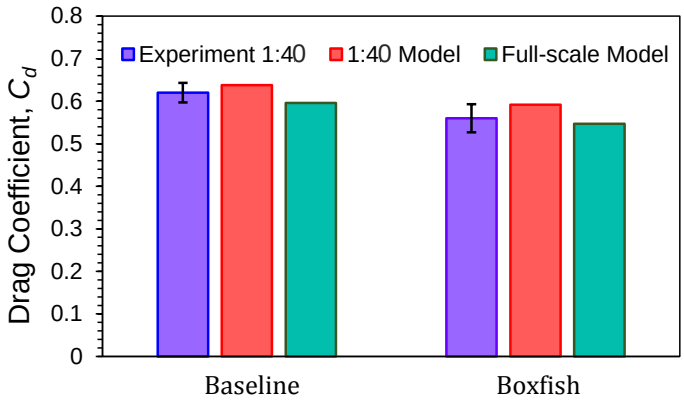

Figure 22: Drag Coefficient Comparison

The drag coefficient results are all in good agreement for the respective designs. The drag coefficients obtained from the full-scale simulations are similar to the wind tunnel results, which indicates that the drag reductions measured at the 1:40 scale might be scalable to full size.

5.0 CONCLUSION

The purpose of this thesis was to provide a new pathway towards reducing aerodynamic drag on tractor-trailers. The new pathway focused on the design of the trailer sidewalls, an option that has been largely overlooked. The results included in this thesis were drag and pressure measurements from a 1:40 scale tractor-trailer model, as wells as 1:40 scale and full-scale numerical simulations.

5.1 CONTRIBUTIONS

This thesis has shown that altering the design of the trailer sidewalls is a pathway worthy of further investigation for reducing drag on tractor-trailers. Results showed drag coefficient reduction by 12.9% in wind tunnel experiments. A 12.9% reduction in drag could improve tractor-trailer fuel economy by 2.8% from 2.5 kilometers per liter (5.8 miles per gallon) to 2.8 kilometers per liter (6.0 miles per gallon) and decrease tractor-trailer fuel

consumption by 2.7%. If the 12.9% drag reduction was implemented across the U.S. fleet of tractor-trailers, 3 billion liters (780 million gallons) of fuel could be saved each year. The reduced fuel consumption would result in lower fuel costs and greenhouse gas emissions.

5.2 ADDITIONAL APPLICATIONS

In addition to use on tractor-trailers, this technology could be used on other transportation systems. For instance, the developed sidewall designs could be potentially useful on single-axle freight trucks and vans, freight trains, and buses.

5.3 FUTURE WORK

Additional work that must be done to further develop this technology includes the optimization of the design of the sidewalls. The designs used for the sidewalls in this thesis did not pass through an iterative design process whereby dimensions of features would be incrementally altered until the optimal dimensions were discovered. Full-scale physical experiments must also be conducted in order to validate that this technology is feasible.

5.4 SUMMARY

In conclusion, society would benefit from improvements to fuel economy of tractor-trailers. This research has shown that bio-inspired trailer sidewall designs are a promising new pathway for achieving improved tractor-trailer fuel economy. This work should continue to be pursued so that it may one day potentially provide benefits to society.

APPENDIX A: PATENT REVIEW

Results of Search in US Patent Collection Database for:

"drag reduction" AND "tractor-trailer"

Result No.	PAT. NO.	Title	Bio-Inspired Trailer Design for Aerodynamic Drag Reduction?
1	9573635	Aerodynamic drag reducing apparatus	No
2	9567017	Active modular aerodynamic drag reduction system	No
3	9567016	Wheel fairing deflecting wind onto lower wheel	No
4	9527534	Systems and methods for reducing aerodynamic drag on cargo trucks	No
5	9522379	Reducing and/or harvesting drag energy from transport vehicles, including for chemical reactors, and associated systems and methods	No
6	9505449	Apparatuses, assemblies, and methods for drag reduction of land vehicles	No
7	9481407	Drag reduction system	No
8	9481406	Drag reduction device and a vehicle comprising the device	No
9	9457847	Rear-mounted aerodynamic structures for cargo bodies	No

Result No.	PAT. NO.	Title	Bio-Inspired Trailer Design for Aerodynamic Drag Reduction?
10	9428228	Drag reducing mirror assemblies for vehicles	No
11	9389613	Determining turning radius of coupled vehicles	No
12	9333993	Self-deploying apparatuses, assemblies, and methods for drag reduction of land vehicles	No
13	9283997	Multicomponent improved vehicle fuel economy system	No
14	9283996	Airflow baffle for commerical truck fuel efficiency improvements	No
15	9211919	Aerodynamic trucking systems	No
16	9205778	Drag reducing mirror assemblies for vehicles	No
17	9199676	Side skirt system for a trailer	No
18	9199675	Corner coupled vortex structures, trailers, and vehicles including the same	No
19	9199673	Aerodynamic rear drag reduction system for a trailer	No
20	9193399	Active and passive boundary layer control for vehicle drag reduction	No

Result No.	PAT. NO.	Title	Bio-Inspired Trailer Design for Aerodynamic Drag Reduction?
21	9162716	Retractable air deflection apparatus for reduction of vehicular air drag	No
22	9139241	Vehicle drag reduction device	No
23	9139238	Drag reduction of a tractor-trailer using guide vanes	No
24	9132869	Aerodynamic drag reduction system	No
25	9126638	Aerodynamic drag reducing apparatus	No
26	9090294	Aerodynamic fairings for trailers	No
27	9079622	Gap fairing for a tractor-trailer	No
28	9056636	Devices and methods for reducing vehicle drag	No
29	8985677	Vehicle fuel economy system	No
30	8967311	Directed gas systems for improving aerodynamics of a vehicle in cross wind conditions	No
31	8950534	Directed air systems for improving aerodynamics of a vehicle	No

Result No.	PAT. NO.	Title	Bio-Inspired Trailer Design for Aerodynamic Drag Reduction?
32	8944490	Undercarriage fairings for trailers	No
33	8939517	Textile cover for streamlining wide based truck or bus wheels	No
34	8919863	Drag reduction plate and structure for trailers	No
35	8911703	Reducing and/or harvesting drag energy from transport vehicles, including for chemical reactors, and associated systems and methods	No
36	8911000	Retractable air deflection apparatus for reduction of vehicular air drag	No
37	8899659	Recess steps for cab access	No
38	8870275	Active and passive boundary layer control for vehicle drag reduction	No
39	8851554	Vehicle drag reduction assembly	No
40	8845007	Drag reducing device	No
41	8827351	Tractor-trailer cross wind blocker	No
42	8820817	Tractor-trailer rear door air drag reduction system to reduce fuel consumption	No

Result No.	PAT. NO.	Title	Bio-Inspired Trailer Design for Aerodynamic Drag Reduction?
43	8801078	Side skirt system for a trailer	No
44	8783788	Method of covering a wheel for decoration, streamlining, or advertising display, and a flexible wheel cover therefor	No
45	8783758	Folding side skirt system for a trailer	No
46	8783757	Devices and methods for reducing vehicle drag	No
47	8777297	Airflow baffle for commercial truck fuel efficiency improvements	No
48	8770650	Variable geometry aerodynamic fairing for reducing base drag of tractor-trailers	No
49	8770649	Device, assembly, and system for reducing aerodynamic drag	No
50	8757701	Drag reduction device for transport vehicles having randomized irregular shaped edge vortex generating channels	No
51	8746779	Tri-wing system for reduction of the aerodynamic drag of ground vehicles	No
52	8733954	Devices and methods for reducing vehicle drag	No
53	8727425	Aerodynamic trucking systems	No

Result No.	PAT. NO.	Title	Bio-Inspired Trailer Design for Aerodynamic Drag Reduction?
54	8696047	Retractable air deflection apparatus for reduction of vehicular air drag	No
55	8684448	Aerodynamic fairings for trailers	No
56	8684447	Devices and methods for reducing vehicle drag	No
57	8678473	Aerodynamic component mounting assembly for tractor-trailer	No
58	8641126	Sealed aft cavity drag reducer	No
59	8627913	System and method to reduce the aerodynamic force on a vehicle	No
60	8622462	Drag reducing apparatus for a vehicle	No
61	8616616	Side skirt for a pulled vehicle	No
62	8608228	Drag-reducing device	No
63	8590961	Aerodynamic drag reducing apparatus	No
64	8579360	Apparatus for reducing drag on a vehicle	No

Result No.	PAT. NO.	Title	Bio-Inspired Trailer Design for Aerodynamic Drag Reduction?
65	8579359	Side skirt system for a trailer	No
66	8579357	Retractable air deflection apparatus for reduction of vehicular air drag	No
67	8550540	Aerodynamic device for trailers and the like	No
68	8550539	Aerodynamic drag reducer for vehicles	No
69	8517452	Tractor-trailer cross wind blocker	No
70	8506004	Gap fairing and drag reduction method	No
71	8500291	Devices and methods for reducing vehicle drag	No
72	8491036	Devices and methods for reducing vehicle drag	No
73	8491035	Aerodynamic drag reduction apparatus for a trailer	No
74	8444210	Drag reducing apparatus for a vehicle	No
75	8414064	Apparatus for reducing drag on a vehicle	No

Result No.	PAT. NO.	Title	Bio-Inspired Trailer Design for Aerodynamic Drag Reduction?
76	8398150	Side skirt system for a trailer	No
77	8382210	Wheel cover with window for over-the-road trucks, trailers and the like	No
78	8382194	Outboard wake stabilization device and method for reducing the aerodynamic drag of ground vehicles	No
79	8360507	Apparatus for reducing drag on a vehicle	No
80	8342595	Devices and methods for reducing vehicle drag	No
81	8342594	Apparatus for reducing drag on a vehicle	No
82	8303025	Aerodynamic trucking systems	No
83	8287030	Drag reducing apparatus for a vehicle	No
84	8276972	Undercarriage fairing	No
85	8267211	System and method to reduce the aerodynamic force on a vehicle	No
86	8251436	Devices and methods for reducing vehicle drag	No

Result No.	PAT. NO.	Title	Bio-Inspired Trailer Design for Aerodynamic Drag Reduction?
87	8235456	Retractable air deflection apparatus for reduction of vehicular air drag	No
88	8210599	Aerodynamic and protective vehicle panel assembly and method of constructing same	No
89	8196994	Rotationally supporting structure of vehicle's drag-reducing apparatus	No
90	8196993	Drag reducing deflector	No
91	8177287	Self-deploying drag reducing device	No
92	8177286	Side skirt system for a trailer	No
93	8162384	Side underride cable system for a trailer	No
94	8162381	Inflatable drag reduction device for vehicles	No
95	8136868	Retractable air deflection apparatus for reduction of vehicular air drag	No
96	8133293	Air cleaner boattail	No
97	8091950	Methods and apparatus for reducing drag via a plasma actuator	No

Result No.	PAT. NO.	Title	Bio-Inspired Trailer Design for Aerodynamic Drag Reduction?
98	8079634	Sealed AFT cavity drag reducer	No
99	8033594	Retractable air deflection apparatus for reduction of vehicular air drag	No
100	8025330	Vehicle fairing structure	No
101	8007030	Frame extension device for reducing the aerodynamic drag of ground vehicles	No
102	7992666	System and method to reduce the aerodynamic force on a vehicle	No
103	7976096	Air drag reduction apparatus for tractor-trailers	No
104	7958966	Exhaust stack fairing	No
105	7950720	Apparatus for reducing drag on vehicles with planar rear surfaces	No
106	7866734	Inflatable shaping system reducing the aerodynamic drag upon the rear of a vehicle	No
107	7862102	Apparatus for reducing drag on vehicles	No
108	7857376	Aerodynamic drag reducing apparatus	No

Result No.	PAT. NO.	Title	Bio-Inspired Trailer Design for Aerodynamic Drag Reduction?
109	7854468	Self-deploying drag reducing device	No
110	7837254	Vehicle fairing structure	No
111	7828368	Vehicle underbody fairing	No
112	7789453	Trailer keel	No
113	7780224	Crash attenuating underride guard	No
114	7765044	Drag reducing system	No
115	7748771	Apparatus to improve the aerodynamics, fuel economy, docking and handling of heavy trucks	No
116	7740303	Mini skirt aerodynamic fairing device for reducing the aerodynamic drag of ground vehicles	No
117	7699382	Trailer with aerodynamic rear door	No
118	7694774	Reduced wind resistant haulage vehicle apparatus	No
119	7665797	Braced fairing for drag and vibration reduction of round tubing	No

Result No.	PAT. NO.	Title	Bio-Inspired Trailer Design for Aerodynamic Drag Reduction?
120	7641262	Retractable air deflection apparatus for reduction of vehicular air drag	No
121	7585015	Frame extension device for reducing the aerodynamic drag of ground vehicles	No
122	7578541	Trailer skirt panel	No
123	7537270	Air foil	No
124	7497502	Mini skirt aerodynamic fairing device for reducing the aerodynamic drag of ground vehicles	No
125	7431381	Wake stabilization device and method for reducing the aerodynamic drag of ground vehicles	No
126	7364220	Aerodynamic drag reduction systems	No
127	7318620	Flexible cross flow vortex trap device for reducing the aerodynamic drag of ground vehicles	No
128	7255387	Vortex strake device and method for reducing the aerodynamic drag of ground vehicles	No
129	7243980	Vehicle drag reduction apparatus	No
130	7237827	Control system for pressure drag reduction system	No

Result No.	PAT. NO.	Title	Bio-Inspired Trailer Design for Aerodynamic Drag Reduction?
131	7216923	Systems and methods for reducing the aerodynamic drag on vehicles	No
132	7207620	Aerodynamic drag reducing system with retrofittable, selectively removable frame	No
133	7202776	Method and system for detecting objects external to a vehicle	No
134	7192077	Vehicle drag reduction with air scoop vortex impeller and trailing edge surface texture treatment	No
135	7185944	Pressure drag reduction system with an internal duct	No
136	7165804	Methods for reducing the aerodynamic drag of vehicles	No
137	7156453	Pressure drag reduction system with a side duct	No
138	7152908	Systems, methods, and media for reducing the aerodynamic drag of vehicles	No
139	7085637	Method and system for controlling a vehicle	No
140	7073845	Aerodynamic drag reduction apparatus for gap-divided bluff bodies such as tractor-trailers	No
141	7008004	Boattail plates with non-rectangular geometries for reducing aerodynamic base drag of a bluff body in ground effect	No

Result No.	PAT. NO.	Title	Bio-Inspired Trailer Design for Aerodynamic Drag Reduction?
142	6986544	Cross flow vortex trap device and method for reducing the aerodynamic drag of ground vehicles	No
143	6979049	Apparatus and method for reducing drag of a bluff body in ground effect using counter-rotating vortex pairs	No
144	6974178	Aerodynamic drag reduction apparatus for wheeled vehicles in ground effect	No
145	6959958	Aerodynamic combination for improved base drag reduction	No
146	6926345	Apparatus and method for reducing drag of a bluff body in ground effect using counter-rotating vortex pairs	No
147	6899369	Method and apparatus for reducing drag on a vehicle in motion and channeling air flow to form a bug shield	No
148	6790526	Oxyhalopolymer protective multifunctional appliques and paint replacement films	No
149	6789839	Wind dam for use with tractor-trailers	No
150	6779834	Drag reduction channel apparatus for roadway vehicles	No
151	6768944	Method and system for controlling a vehicle	No
152	6742616	Hybrid air boost vehicle and method for making same	No

Result No.	PAT. NO.	Title	Bio-Inspired Trailer Design for Aerodynamic Drag Reduction?
153	6720920	Method and arrangement for communicating between vehicles	No
154	6702364	Method and apparatus for reducing drag on a vehicle in motion and channeling air flow to form a bug shield	No
155	6685256	Trailer drag reduction system	No
156	6666498	Deployable airfoil for trucks and trailers	No
157	6616218	Base passive porosity for vehicle drag reduction	No
158	6461218	Remotely controlled toy motorized snake	No
159	6409252	Truck trailer drag reducer	No
160	6286894	Reduced-drag trailer	No
161	6286892	Base passive porosity for drag reduction	No
162	6257654	Air drag reducing apparatus	No
163	6204820	Antenna mount for air drag reduction equipment for motor vehicles	No

Result No.	PAT. NO.	Title	Bio-Inspired Trailer Design for Aerodynamic Drag Reduction?
164	6068328	Vehicular boundary layer control system and method	No
165	5947548	Aerodynamic drag reducing geometry for land-based vehicles	No
166	5755485	Rooftop drag reducing device	No
167	5375903	Device for reducing the aerodynamic resistance of a commercial vehicle	No
168	5374013	Method and apparatus for reducing drag on a moving body	No
169	5348366	Drag reducing device for land vehicles	No
170	5289997	Apparatus and method for reducing drag on bodies moving through fluid	No
171	5280990	Vehicle drag reduction system	No
172	5190342	Tractor-trailer aerodynamic drag reduction apparatus and method	No
173	5174626	Rooftop drag reducing device	No
174	5108145	Apparatus and method for motor vehicle air drag reduction using rear surface structure	No

Result No.	PAT. NO.	Title	Bio-Inspired Trailer Design for Aerodynamic Drag Reduction?
175	5058945	Long-haul vehicle streamline apparatus	No
176	4867397	Vehicle aerodynamic drag reduction system and process	No
177	4813635	Projectile with reduced base drag	No
178	4813633	Airfoil trailing edge	No
179	4789117	Bodies with reduced base drag	No
180	4776535	Convoluted plate to reduce base drag	No
181	4756256	Aerodynamic drag reduction for railcars	No
182	4741569	Inflatable drag reducer for land transport vehicles	No
183	4702509	Long-haul vehicle streamline apparatus	No
184	4688841	Drag reduction device for tractor-trailers	No
185	4611847	Inflatable and extendable vehicle skirt	No

Result No.	PAT. NO.	Title	Bio-Inspired Trailer Design for Aerodynamic Drag Reduction?
186	4511170	Aerodynamic device for land vehicles	No
187	4508380	Truck afterbody drag reducing device	No
188	4486046	Undercarriage airstream deflector assembly for truck trailers and the like	No
189	4457550	Means for reducing vehicle drag	No
190	4375898	Air deflector assembly	No
191	4360232	Aerodynamic drag reduction apparatus for vehicles or the like	No
192	4313635	Wind deflector system for aerodynamic drag reduction	No
193	4311334	Universal towed vehicle wind umbrella	No
194	4257641	Vehicle drag reducer	No
195	4257640	Drag reducer for land vehicles	No
196	4245862	Drag reducer for land vehicles	No

Result No.	PAT. NO.	Title	Bio-Inspired Trailer Design for Aerodynamic Drag Reduction?
197	4210354	Aerodynamic drag-reducing shield for mounting on the front of a cargo carrying compartment of a road vehicle	No
198	4102548	Infinitely variable, controllably and/or automatically adjustable air deflector and method	No
199	4068883	Wind deflector configuration	No
200	4056279	Air deflector for tractor-trailer vehicle	No
201	4035013	Drag reducer for land vehicles	No
202	4030779	Inflatable streamlining structure for vehicles	No
203	4022508	Air drag reducing means for bluff vehicles and the like	No
204	4021069	Apparatus for reducing aerodynamic drag	No
205	3977716	Wind drag reducer for towed vehicles	No
206	3972556	Tractor-trailer aerodynamic drag reducer	No
207	3971586	Drag reducer for land vehicles	No

Result No.	PAT. NO.	Title	Bio-Inspired Trailer Design for Aerodynamic Drag Reduction?
208	3951445	Drag reduction apparatus and method	No
209	3934923	Air decelerator for truck cab	No

APPENDIX B: DRAG DATA PROCESSING WITH MATLAB

```
close all
clear
clc
format shortE

%Import Drag Experiment Data from 3/3/2016
fid=fopen('20160303.txt');
data1=textscan(fid,'%f %f %f');
fclose(fid);
data1=cell2mat(data1);

%Import Drag Experiment Data from 3/4/2016
fid=fopen('20160304.txt');
data2=textscan(fid,'%f %f %f');
fclose(fid);
data2=cell2mat(data2);

%Import Drag Experiment Data from 3/5/2016
fid=fopen('20160305.txt');
data3=textscan(fid,'%f %f %f');
fclose(fid);
data3=cell2mat(data3);

%Compile All Drag Experiment Data into 1 Matrix
data=vertcat(data1,data2,data3);
[m,n]=size(data);

%Create Load Cell Output Voltage Vectors [Volts]
baseline_40_vo=[];
boxfish_40_vo=[];
shark_40_vo=[];
combined_40_vo=[];
baseline_45_vo=[];
boxfish_45_vo=[];
shark_45_vo=[];
combined_45_vo=[];
baseline_50_vo=[];
boxfish_50_vo=[];
shark_50_vo=[];
combined_50_vo=[];
baseline_55_vo=[];
boxfish_55_vo=[];
shark_55_vo=[];
combined_55_vo=[];
baseline_60_vo=[];
boxfish_60_vo=[];
shark_60_vo=[];
combined_60_vo=[];
baseline_65_vo=[];
boxfish_65_vo=[];
```

```
shark_65_vo=[];
combined_65_vo=[];
baseline_70_vo=[];
boxfish_70_vo=[];
shark_70_vo=[];
combined_70_vo=[];
baseline_75_vo=[];
boxfish_75_vo=[];
shark_75_vo=[];
combined_75_vo=[];
baseline_80_vo=[];
boxfish_80_vo=[];
shark_80_vo=[];
combined_80_vo=[];
baseline_85_vo=[];
boxfish_85_vo=[];
shark_85_vo=[];
combined_85_vo=[];
for i=1:m
    if data(i,1)==1 && data(i,2)==40
        baseline_40_vo=vertcat(baseline_40_vo,data(i,3));
    end
    if data(i,1)==1 && data(i,2)==45
        baseline_45_vo=vertcat(baseline_45_vo,data(i,3));
    end
    if data(i,1)==1 && data(i,2)==50
        baseline_50_vo=vertcat(baseline_50_vo,data(i,3));
    end
    if data(i,1)==1 && data(i,2)==55
        baseline_55_vo=vertcat(baseline_55_vo,data(i,3));
    end
    if data(i,1)==1 && data(i,2)==60
        baseline_60_vo=vertcat(baseline_60_vo,data(i,3));
    end
    if data(i,1)==1 && data(i,2)==65
        baseline_65_vo=vertcat(baseline_65_vo,data(i,3));
    end
    if data(i,1)==1 && data(i,2)==70
        baseline_70_vo=vertcat(baseline_70_vo,data(i,3));
    end
    if data(i,1)==1 && data(i,2)==75
        baseline_75_vo=vertcat(baseline_75_vo,data(i,3));
    end
    if data(i,1)==1 && data(i,2)==80
        baseline_80_vo=vertcat(baseline_80_vo,data(i,3));
    end
    if data(i,1)==1 && data(i,2)==85
        baseline_85_vo=vertcat(baseline_85_vo,data(i,3));
    end
    if data(i,1)==3 && data(i,2)==40
        boxfish_40_vo=vertcat(boxfish_40_vo,data(i,3));
    end
    if data(i,1)==3 && data(i,2)==45
        boxfish_45_vo=vertcat(boxfish_45_vo,data(i,3));
```

```
    end
    if data(i,1)==3 && data(i,2)==50
        boxfish_50_vo=vertcat(boxfish_50_vo,data(i,3));
    end
    if data(i,1)==3 && data(i,2)==55
        boxfish_55_vo=vertcat(boxfish_55_vo,data(i,3));
    end
    if data(i,1)==3 && data(i,2)==60
        boxfish_60_vo=vertcat(boxfish_60_vo,data(i,3));
    end
    if data(i,1)==3 && data(i,2)==65
        boxfish_65_vo=vertcat(boxfish_65_vo,data(i,3));
    end
    if data(i,1)==3 && data(i,2)==70
        boxfish_70_vo=vertcat(boxfish_70_vo,data(i,3));
    end
    if data(i,1)==3 && data(i,2)==75
        boxfish_75_vo=vertcat(boxfish_75_vo,data(i,3));
    end
    if data(i,1)==3 && data(i,2)==80
        boxfish_80_vo=vertcat(boxfish_80_vo,data(i,3));
    end
    if data(i,1)==3 && data(i,2)==85
        boxfish_85_vo=vertcat(boxfish_85_vo,data(i,3));
    end
    if data(i,1)==2 && data(i,2)==40
        shark_40_vo=vertcat(shark_40_vo,data(i,3));
    end
    if data(i,1)==2 && data(i,2)==45
        shark_45_vo=vertcat(shark_45_vo,data(i,3));
    end
    if data(i,1)==2 && data(i,2)==50
        shark_50_vo=vertcat(shark_50_vo,data(i,3));
    end
    if data(i,1)==2 && data(i,2)==55
        shark_55_vo=vertcat(shark_55_vo,data(i,3));
    end
    if data(i,1)==2 && data(i,2)==60
        shark_60_vo=vertcat(shark_60_vo,data(i,3));
    end
    if data(i,1)==2 && data(i,2)==65
        shark_65_vo=vertcat(shark_65_vo,data(i,3));
    end
    if data(i,1)==2 && data(i,2)==70
        shark_70_vo=vertcat(shark_70_vo,data(i,3));
    end
    if data(i,1)==2 && data(i,2)==75
        shark_75_vo=vertcat(shark_75_vo,data(i,3));
    end
    if data(i,1)==2 && data(i,2)==80
        shark_80_vo=vertcat(shark_80_vo,data(i,3));
    end
    if data(i,1)==2 && data(i,2)==85
        shark_85_vo=vertcat(shark_85_vo,data(i,3));
```

```
    end
    if data(i,1)==4 && data(i,2)==40
        combined_40_vo=vertcat(combined_40_vo,data(i,3));
    end
    if data(i,1)==4 && data(i,2)==45
        combined_45_vo=vertcat(combined_45_vo,data(i,3));
    end
    if data(i,1)==4 && data(i,2)==50
        combined_50_vo=vertcat(combined_50_vo,data(i,3));
    end
    if data(i,1)==4 && data(i,2)==55
        combined_55_vo=vertcat(combined_55_vo,data(i,3));
    end
    if data(i,1)==4 && data(i,2)==60
        combined_60_vo=vertcat(combined_60_vo,data(i,3));
    end
    if data(i,1)==4 && data(i,2)==65
        combined_65_vo=vertcat(combined_65_vo,data(i,3));
    end
    if data(i,1)==4 && data(i,2)==70
        combined_70_vo=vertcat(combined_70_vo,data(i,3));
    end
    if data(i,1)==4 && data(i,2)==75
        combined_75_vo=vertcat(combined_75_vo,data(i,3));
    end
    if data(i,1)==4 && data(i,2)==80
        combined_80_vo=vertcat(combined_80_vo,data(i,3));
    end
    if data(i,1)==4 && data(i,2)==85
        combined_85_vo=vertcat(combined_85_vo,data(i,3));
    end
end

%Calculate Drag Force Vectors [Newtons]
baseline_40_fd=(baseline_40_vo-0.5)*25/4*9.80665*0.45359237*1.1875/(16.75+4.50613315/2);
boxfish_40_fd=(boxfish_40_vo-0.5)*25/4*9.80665*0.45359237*1.1875/(16.75+4.50613315/2);
shark_40_fd=(shark_40_vo-0.5)*25/4*9.80665*0.45359237*1.1875/(16.75+4.50613315/2);
combined_40_fd=(combined_40_vo-0.5)*25/4*9.80665*0.45359237*1.1875/(16.75+4.50613315/2);
baseline_45_fd=(baseline_45_vo-0.5)*25/4*9.80665*0.45359237*1.1875/(16.75+4.50613315/2);
boxfish_45_fd=(boxfish_45_vo-0.5)*25/4*9.80665*0.45359237*1.1875/(16.75+4.50613315/2);
shark_45_fd=(shark_45_vo-0.5)*25/4*9.80665*0.45359237*1.1875/(16.75+4.50613315/2);
combined_45_fd=(combined_45_vo-0.5)*25/4*9.80665*0.45359237*1.1875/(16.75+4.50613315/2);
baseline_50_fd=(baseline_50_vo-0.5)*25/4*9.80665*0.45359237*1.1875/(16.75+4.50613315/2);
boxfish_50_fd=(boxfish_50_vo-0.5)*25/4*9.80665*0.45359237*1.1875/(16.75+4.50613315/2);
shark_50_fd=(shark_50_vo-0.5)*25/4*9.80665*0.45359237*1.1875/(16.75+4.50613315/2);
combined_50_fd=(combined_50_vo-0.5)*25/4*9.80665*0.45359237*1.1875/(16.75+4.50613315/2);
baseline_55_fd=(baseline_55_vo-0.5)*25/4*9.80665*0.45359237*1.1875/(16.75+4.50613315/2);
boxfish_55_fd=(boxfish_55_vo-0.5)*25/4*9.80665*0.45359237*1.1875/(16.75+4.50613315/2);
shark_55_fd=(shark_55_vo-0.5)*25/4*9.80665*0.45359237*1.1875/(16.75+4.50613315/2);
combined_55_fd=(combined_55_vo-0.5)*25/4*9.80665*0.45359237*1.1875/(16.75+4.50613315/2);
baseline_60_fd=(baseline_60_vo-0.5)*25/4*9.80665*0.45359237*1.1875/(16.75+4.50613315/2);
boxfish_60_fd=(boxfish_60_vo-0.5)*25/4*9.80665*0.45359237*1.1875/(16.75+4.50613315/2);
shark_60_fd=(shark_60_vo-0.5)*25/4*9.80665*0.45359237*1.1875/(16.75+4.50613315/2);
combined_60_fd=(combined_60_vo-0.5)*25/4*9.80665*0.45359237*1.1875/(16.75+4.50613315/2);
```

```
baseline_65_fd=(baseline_65_vo-0.5)*25/4*9.80665*0.45359237*1.1875/(16.75+4.50613315/2);
boxfish_65_fd=(boxfish_65_vo-0.5)*25/4*9.80665*0.45359237*1.1875/(16.75+4.50613315/2);
shark_65_fd=(shark_65_vo-0.5)*25/4*9.80665*0.45359237*1.1875/(16.75+4.50613315/2);
combined_65_fd=(combined_65_vo-0.5)*25/4*9.80665*0.45359237*1.1875/(16.75+4.50613315/2);
baseline_70_fd=(baseline_70_vo-0.5)*25/4*9.80665*0.45359237*1.1875/(16.75+4.50613315/2);
boxfish_70_fd=(boxfish_70_vo-0.5)*25/4*9.80665*0.45359237*1.1875/(16.75+4.50613315/2);
shark_70_fd=(shark_70_vo-0.5)*25/4*9.80665*0.45359237*1.1875/(16.75+4.50613315/2);
combined_70_fd=(combined_70_vo-0.5)*25/4*9.80665*0.45359237*1.1875/(16.75+4.50613315/2);
baseline_75_fd=(baseline_75_vo-0.5)*25/4*9.80665*0.45359237*1.1875/(16.75+4.50613315/2);
boxfish_75_fd=(boxfish_75_vo-0.5)*25/4*9.80665*0.45359237*1.1875/(16.75+4.50613315/2);
shark_75_fd=(shark_75_vo-0.5)*25/4*9.80665*0.45359237*1.1875/(16.75+4.50613315/2);
combined_75_fd=(combined_75_vo-0.5)*25/4*9.80665*0.45359237*1.1875/(16.75+4.50613315/2);
baseline_80_fd=(baseline_80_vo-0.5)*25/4*9.80665*0.45359237*1.1875/(16.75+4.50613315/2);
boxfish_80_fd=(boxfish_80_vo-0.5)*25/4*9.80665*0.45359237*1.1875/(16.75+4.50613315/2);
shark_80_fd=(shark_80_vo-0.5)*25/4*9.80665*0.45359237*1.1875/(16.75+4.50613315/2);
combined_80_fd=(combined_80_vo-0.5)*25/4*9.80665*0.45359237*1.1875/(16.75+4.50613315/2);
baseline_85_fd=(baseline_85_vo-0.5)*25/4*9.80665*0.45359237*1.1875/(16.75+4.50613315/2);
boxfish_85_fd=(boxfish_85_vo-0.5)*25/4*9.80665*0.45359237*1.1875/(16.75+4.50613315/2);
shark_85_fd=(shark_85_vo-0.5)*25/4*9.80665*0.45359237*1.1875/(16.75+4.50613315/2);
combined_85_fd=(combined_85_vo-0.5)*25/4*9.80665*0.45359237*1.1875/(16.75+4.50613315/2);

%Define Cross Sectional Areas [m^2]
baseline_a=0.006516116;
boxfish_a=0.006870954;
shark_a=0.006645148;
combined_a=0.0071483728;

%Calculate Drag Coefficient Vectors
baseline_40_cd=(baseline_40_fd.*2./1.225./(40.*5280.*12.*.0254./60./60).^2./baseline_a);
boxfish_40_cd=(boxfish_40_fd.*2./1.225./(40.*5280.*12.*.0254./60./60).^2./boxfish_a);
shark_40_cd=(shark_40_fd.*2./1.225./(40.*5280.*12.*.0254./60./60).^2./shark_a);
combined_40_cd=(combined_40_fd.*2./1.225./(40.*5280.*12.*.0254./60./60).^2./combined_a);
baseline_45_cd=(baseline_45_fd.*2./1.225./(45.*5280.*12.*.0254./60./60).^2./baseline_a);
boxfish_45_cd=(boxfish_45_fd.*2./1.225./(45.*5280.*12.*.0254./60./60).^2./boxfish_a);
shark_45_cd=(shark_45_fd.*2./1.225./(45.*5280.*12.*.0254./60./60).^2./shark_a);
combined_45_cd=(combined_45_fd.*2./1.225./(45.*5280.*12.*.0254./60./60).^2./combined_a);
baseline_50_cd=(baseline_50_fd.*2./1.225./(50.*5280.*12.*.0254./60./60).^2./baseline_a);
boxfish_50_cd=(boxfish_50_fd.*2./1.225./(50.*5280.*12.*.0254./60./60).^2./boxfish_a);
shark_50_cd=(shark_50_fd.*2./1.225./(50.*5280.*12.*.0254./60./60).^2./shark_a);
combined_50_cd=(combined_50_fd.*2./1.225./(50.*5280.*12.*.0254./60./60).^2./combined_a);
baseline_55_cd=(baseline_55_fd.*2./1.225./(55.*5280.*12.*.0254./60./60).^2./baseline_a);
boxfish_55_cd=(boxfish_55_fd.*2./1.225./(55.*5280.*12.*.0254./60./60).^2./boxfish_a);
shark_55_cd=(shark_55_fd.*2./1.225./(55.*5280.*12.*.0254./60./60).^2./shark_a);
combined_55_cd=(combined_55_fd.*2./1.225./(55.*5280.*12.*.0254./60./60).^2./combined_a);
baseline_60_cd=(baseline_60_fd.*2./1.225./(60.*5280.*12.*.0254./60./60).^2./baseline_a);
boxfish_60_cd=(boxfish_60_fd.*2./1.225./(60.*5280.*12.*.0254./60./60).^2./boxfish_a);
shark_60_cd=(shark_60_fd.*2./1.225./(60.*5280.*12.*.0254./60./60).^2./shark_a);
combined_60_cd=(combined_60_fd.*2./1.225./(60.*5280.*12.*.0254./60./60).^2./combined_a);
baseline_65_cd=(baseline_65_fd.*2./1.225./(65.*5280.*12.*.0254./60./60).^2./baseline_a);
boxfish_65_cd=(boxfish_65_fd.*2./1.225./(65.*5280.*12.*.0254./60./60).^2./boxfish_a);
shark_65_cd=(shark_65_fd.*2./1.225./(65.*5280.*12.*.0254./60./60).^2./shark_a);
combined_65_cd=(combined_65_fd.*2./1.225./(65.*5280.*12.*.0254./60./60).^2./combined_a);
baseline_70_cd=(baseline_70_fd.*2./1.225./(70.*5280.*12.*.0254./60./60).^2./baseline_a);
boxfish_70_cd=(boxfish_70_fd.*2./1.225./(70.*5280.*12.*.0254./60./60).^2./boxfish_a);
```

```
shark_70_cd=(shark_70_fd.*2./1.225./(70.*5280.*12.*.0254./60./60).^2./shark_a);
combined_70_cd=(combined_70_fd.*2./1.225./(70.*5280.*12.*.0254./60./60).^2./combined_a);
baseline_75_cd=(baseline_75_fd.*2./1.225./(75.*5280.*12.*.0254./60./60).^2./baseline_a);
boxfish_75_cd=(boxfish_75_fd.*2./1.225./(75.*5280.*12.*.0254./60./60).^2./boxfish_a);
shark_75_cd=(shark_75_fd.*2./1.225./(75.*5280.*12.*.0254./60./60).^2./shark_a);
combined_75_cd=(combined_75_fd.*2./1.225./(75.*5280.*12.*.0254./60./60).^2./combined_a);
baseline_80_cd=(baseline_80_fd.*2./1.225./(80.*5280.*12.*.0254./60./60).^2./baseline_a);
boxfish_80_cd=(boxfish_80_fd.*2./1.225./(80.*5280.*12.*.0254./60./60).^2./boxfish_a);
shark_80_cd=(shark_80_fd.*2./1.225./(80.*5280.*12.*.0254./60./60).^2./shark_a);
combined_80_cd=(combined_80_fd.*2./1.225./(80.*5280.*12.*.0254./60./60).^2./combined_a);
baseline_85_cd=(baseline_85_fd.*2./1.225./(85.*5280.*12.*.0254./60./60).^2./baseline_a);
boxfish_85_cd=(boxfish_85_fd.*2./1.225./(85.*5280.*12.*.0254./60./60).^2./boxfish_a);
shark_85_cd=(shark_85_fd.*2./1.225./(85.*5280.*12.*.0254./60./60).^2./shark_a);
combined_85_cd=(combined_85_fd.*2./1.225./(85.*5280.*12.*.0254./60./60).^2./combined_a);

%Drag Coefficient Box Plots (design 1 is baseline, 2 is boxfish, 3 is shark, 4 is combined)
fntsz=14;
a40=zeros(2997,4);  a40(:,1)=baseline_40_cd;      a40(:,2)=boxfish_40_cd;
a40(:,3)=shark_40_cd;      a40(:,4)=combined_40_cd;
a45=zeros(2997,4);  a45(:,1)=baseline_45_cd;      a45(:,2)=boxfish_45_cd;
a45(:,3)=shark_45_cd;      a45(:,4)=combined_45_cd;
a50=zeros(2997,4);  a50(:,1)=baseline_50_cd;      a50(:,2)=boxfish_50_cd;
a50(:,3)=shark_50_cd;      a50(:,4)=combined_50_cd;
a55=zeros(2997,4);  a55(:,1)=baseline_55_cd;      a55(:,2)=boxfish_55_cd;
a55(:,3)=shark_55_cd;      a55(:,4)=combined_55_cd;
a60=zeros(2997,4);  a60(:,1)=baseline_60_cd;      a60(:,2)=boxfish_60_cd;
a60(:,3)=shark_60_cd;      a60(:,4)=combined_60_cd;
a65=zeros(2997,4);  a65(:,1)=baseline_65_cd;      a65(:,2)=boxfish_65_cd;
a65(:,3)=shark_65_cd;      a65(:,4)=combined_65_cd;
a70=zeros(2997,4);  a70(:,1)=baseline_70_cd;      a70(:,2)=boxfish_70_cd;
a70(:,3)=shark_70_cd;      a70(:,4)=combined_70_cd;
a75=zeros(2997,4);  a75(:,1)=baseline_75_cd;      a75(:,2)=boxfish_75_cd;
a75(:,3)=shark_75_cd;      a75(:,4)=combined_75_cd;
a80=zeros(2997,4);  a80(:,1)=baseline_80_cd;      a80(:,2)=boxfish_80_cd;
a80(:,3)=shark_80_cd;      a80(:,4)=combined_80_cd;
a85=zeros(2997,4);  a85(:,1)=baseline_85_cd;      a85(:,2)=boxfish_85_cd;
a85(:,3)=shark_85_cd;      a85(:,4)=combined_85_cd;
figure(40)
boxplot(a40,'Labels',{'Design - 1','Design - 2','Design - 3','Design -
4'},'Symbol','ro','Whisker',100)
title('40 mph')
ylabel('C_D','fontsize',fntsz)
xlabel('Trailer Design','fontsize',fntsz)
set(gca,'FontSize',fntsz)
saveas(figure(40),'boxplot_cd_40.emf')
figure(45)
boxplot(a45,'Labels',{'Design - 1','Design - 2','Design - 3','Design -
4'},'Symbol','ro','Whisker',100)
title('45 mph')
ylabel('C_D','fontsize',fntsz)
xlabel('Trailer Design','fontsize',fntsz)
set(gca,'FontSize',fntsz)
saveas(figure(45),'boxplot_cd_45.emf')
figure(50)
```

```
boxplot(a50,'Labels',{'Design - 1','Design - 2','Design - 3','Design -
4'},'Symbol','ro','Whisker',100)
title('50 mph')
ylabel('C_D','fontsize',fntsz)
xlabel('Trailer Design','fontsize',fntsz)
set(gca,'FontSize',fntsz)
saveas(figure(50),'boxplot_cd_50.emf')
figure(55)
boxplot(a55,'Labels',{'Design - 1','Design - 2','Design - 3','Design -
4'},'Symbol','ro','Whisker',100)
title('55 mph')
ylabel('C_D','fontsize',fntsz)
xlabel('Trailer Design','fontsize',fntsz)
set(gca,'FontSize',fntsz)
saveas(figure(55),'boxplot_cd_55.emf')
figure(60)
boxplot(a60,'Labels',{'Design - 1','Design - 2','Design - 3','Design -
4'},'Symbol','ro','Whisker',100)
title('60 mph')
ylabel('C_D','fontsize',fntsz)
xlabel('Trailer Design','fontsize',fntsz)
set(gca,'FontSize',fntsz)
saveas(figure(60),'boxplot_cd_60.emf')
figure(65)
boxplot(a65,'Labels',{'Design - 1','Design - 2','Design - 3','Design -
4'},'Symbol','ro','Whisker',100)
title('65 mph')
ylabel('C_D','fontsize',fntsz)
xlabel('Trailer Design','fontsize',fntsz)
set(gca,'FontSize',fntsz)
saveas(figure(65),'boxplot_cd_65.emf')
figure(70)
boxplot(a70,'Labels',{'Design - 1','Design - 2','Design - 3','Design -
4'},'Symbol','ro','Whisker',100)
title('70 mph')
ylabel('C_D','fontsize',fntsz)
xlabel('Trailer Design','fontsize',fntsz)
set(gca,'FontSize',fntsz)
saveas(figure(70),'boxplot_cd_70.emf')
figure(75)
boxplot(a75,'Labels',{'Design - 1','Design - 2','Design - 3','Design -
4'},'Symbol','ro','Whisker',100)
title('75 mph')
ylabel('C_D','fontsize',fntsz)
xlabel('Trailer Design','fontsize',fntsz)
set(gca,'FontSize',fntsz)
saveas(figure(75),'boxplot_cd_75.emf')
figure(80)
boxplot(a80,'Labels',{'Design - 1','Design - 2','Design - 3','Design -
4'},'Symbol','ro','Whisker',100)
title('80 mph')
ylabel('C_D','fontsize',fntsz)
xlabel('Trailer Design','fontsize',fntsz)
set(gca,'FontSize',fntsz)
```

```
saveas(figure(80),'boxplot_cd_80.emf')
figure(85)
boxplot(a85,'Labels',{'Design - 1','Design - 2','Design - 3','Design -
4'},'Symbol','ro','Whisker',100)
title('85 mph')
ylabel('C_D','fontsize',fntsz)
xlabel('Trailer Design','fontsize',fntsz)
set(gca,'FontSize',fntsz)
saveas(figure(85),'boxplot_cd_85.emf')

%Drag Coefficient Summary Statistics
table=zeros(130,1);
i=2;
table(i-1)=40;    table(i)=mean(baseline_40_cd);    table(i+1)=mean(boxfish_40_cd);
table(i+2)=mean(shark_40_cd);    table(i+3)=mean(combined_40_cd); i=i+13;
table(i-1)=45;    table(i)=mean(baseline_45_cd);    table(i+1)=mean(boxfish_45_cd);
table(i+2)=mean(shark_45_cd);    table(i+3)=mean(combined_45_cd); i=i+13;
table(i-1)=50;    table(i)=mean(baseline_50_cd);    table(i+1)=mean(boxfish_50_cd);
table(i+2)=mean(shark_50_cd);    table(i+3)=mean(combined_50_cd); i=i+13;
table(i-1)=55;    table(i)=mean(baseline_55_cd);    table(i+1)=mean(boxfish_55_cd);
table(i+2)=mean(shark_55_cd);    table(i+3)=mean(combined_55_cd); i=i+13;
table(i-1)=60;    table(i)=mean(baseline_60_cd);    table(i+1)=mean(boxfish_60_cd);
table(i+2)=mean(shark_60_cd);    table(i+3)=mean(combined_60_cd); i=i+13;
table(i-1)=65;    table(i)=mean(baseline_65_cd);    table(i+1)=mean(boxfish_65_cd);
table(i+2)=mean(shark_65_cd);    table(i+3)=mean(combined_65_cd); i=i+13;
table(i-1)=70;    table(i)=mean(baseline_70_cd);    table(i+1)=mean(boxfish_70_cd);
table(i+2)=mean(shark_70_cd);    table(i+3)=mean(combined_70_cd); i=i+13;
table(i-1)=75;    table(i)=mean(baseline_75_cd);    table(i+1)=mean(boxfish_75_cd);
table(i+2)=mean(shark_75_cd);    table(i+3)=mean(combined_75_cd); i=i+13;
table(i-1)=80;    table(i)=mean(baseline_80_cd);    table(i+1)=mean(boxfish_80_cd);
table(i+2)=mean(shark_80_cd);    table(i+3)=mean(combined_80_cd); i=i+13;
table(i-1)=85;    table(i)=mean(baseline_85_cd);    table(i+1)=mean(boxfish_85_cd);
table(i+2)=mean(shark_85_cd);    table(i+3)=mean(combined_85_cd); i=6;

table(i)=std(baseline_40_cd);    table(i+1)=std(boxfish_40_cd);    table(i+2)=std(shark_40_cd);
table(i+3)=std(combined_40_cd); i=i+13;
table(i)=std(baseline_45_cd);    table(i+1)=std(boxfish_45_cd);    table(i+2)=std(shark_45_cd);
table(i+3)=std(combined_45_cd); i=i+13;
table(i)=std(baseline_50_cd);    table(i+1)=std(boxfish_50_cd);    table(i+2)=std(shark_50_cd);
table(i+3)=std(combined_50_cd); i=i+13;
table(i)=std(baseline_55_cd);    table(i+1)=std(boxfish_55_cd);    table(i+2)=std(shark_55_cd);
table(i+3)=std(combined_55_cd); i=i+13;
table(i)=std(baseline_60_cd);    table(i+1)=std(boxfish_60_cd);    table(i+2)=std(shark_60_cd);
table(i+3)=std(combined_60_cd); i=i+13;
table(i)=std(baseline_65_cd);    table(i+1)=std(boxfish_65_cd);    table(i+2)=std(shark_65_cd);
table(i+3)=std(combined_65_cd); i=i+13;
table(i)=std(baseline_70_cd);    table(i+1)=std(boxfish_70_cd);    table(i+2)=std(shark_70_cd);
table(i+3)=std(combined_70_cd); i=i+13;
table(i)=std(baseline_75_cd);    table(i+1)=std(boxfish_75_cd);    table(i+2)=std(shark_75_cd);
table(i+3)=std(combined_75_cd); i=i+13;
table(i)=std(baseline_80_cd);    table(i+1)=std(boxfish_80_cd);    table(i+2)=std(shark_80_cd);
table(i+3)=std(combined_80_cd); i=i+13;
table(i)=std(baseline_85_cd);    table(i+1)=std(boxfish_85_cd);    table(i+2)=std(shark_85_cd);
table(i+3)=std(combined_85_cd); i=10;
```

```
table(i)=length(baseline_40_cd);    table(i+1)=length(boxfish_40_cd);
table(i+2)=length(shark_40_cd);    table(i+3)=length(combined_40_cd); i=i+13;
table(i)=length(baseline_45_cd);    table(i+1)=length(boxfish_45_cd);
table(i+2)=length(shark_45_cd);    table(i+3)=length(combined_45_cd); i=i+13;
table(i)=length(baseline_50_cd);    table(i+1)=length(boxfish_50_cd);
table(i+2)=length(shark_50_cd);    table(i+3)=length(combined_50_cd); i=i+13;
table(i)=length(baseline_55_cd);    table(i+1)=length(boxfish_55_cd);
table(i+2)=length(shark_55_cd);    table(i+3)=length(combined_55_cd); i=i+13;
table(i)=length(baseline_60_cd);    table(i+1)=length(boxfish_60_cd);
table(i+2)=length(shark_60_cd);    table(i+3)=length(combined_60_cd); i=i+13;
table(i)=length(baseline_65_cd);    table(i+1)=length(boxfish_65_cd);
table(i+2)=length(shark_65_cd);    table(i+3)=length(combined_65_cd); i=i+13;
table(i)=length(baseline_70_cd);    table(i+1)=length(boxfish_70_cd);
table(i+2)=length(shark_70_cd);    table(i+3)=length(combined_70_cd); i=i+13;
table(i)=length(baseline_75_cd);    table(i+1)=length(boxfish_75_cd);
table(i+2)=length(shark_75_cd);    table(i+3)=length(combined_75_cd); i=i+13;
table(i)=length(baseline_80_cd);    table(i+1)=length(boxfish_80_cd);
table(i+2)=length(shark_80_cd);    table(i+3)=length(combined_80_cd); i=i+13;
table(i)=length(baseline_85_cd);    table(i+1)=length(boxfish_85_cd);
table(i+2)=length(shark_85_cd);    table(i+3)=length(combined_85_cd);

fprintf('SUMMARY STATISTICS\n')
fprintf('|--------|-----------------|-----------------|-----------------|-----------------|\n')
fprintf('|        |    Design 1     |    Design 2     |    Design 3     |    Design 4     |\n')
fprintf('|        |   (Baseline)    |    (Boxfish)    |    (Shark)      |   (Combined)    |\n')
fprintf('| Speed  |  Cd  Stdev  N   |  Cd  Stdev  N   |  Cd  Stdev  N   |  Cd  Stdev  N   |\n')
fprintf('|--------|-----------------|-----------------|-----------------|-----------------|\n|
%2.0f mph | %4.2f            | %4.2f            | %4.2f            | %4.2f            |\n|
|      %5.3f      |      %5.3f      |      %5.3f      |      %5.3f      |\n|        |
%4.0f |            %4.0f |            %4.0f |            %4.0f |\n',table)
fprintf('|--------|-----------------|-----------------|-----------------|-----------------|\n')

%Statistical Hypothesis Test
boxfish_40_h=ttest2(boxfish_40_cd,baseline_40_cd,'Alpha',.01,'Tail','left','Vartype','unequal');
shark_40_h=ttest2(shark_40_cd,baseline_40_cd,'Alpha',.01,'Tail','left','Vartype','unequal');
combined_40_h=ttest2(combined_40_cd,baseline_40_cd,'Alpha',.01,'Tail','left','Vartype','unequal')
;
boxfish_45_h=ttest2(boxfish_45_cd,baseline_45_cd,'Alpha',.01,'Tail','left','Vartype','unequal');
shark_45_h=ttest2(shark_45_cd,baseline_45_cd,'Alpha',.01,'Tail','left','Vartype','unequal');
combined_45_h=ttest2(combined_45_cd,baseline_45_cd,'Alpha',.01,'Tail','left','Vartype','unequal')
;
boxfish_50_h=ttest2(boxfish_50_cd,baseline_50_cd,'Alpha',.01,'Tail','left','Vartype','unequal');
shark_50_h=ttest2(shark_50_cd,baseline_50_cd,'Alpha',.01,'Tail','left','Vartype','unequal');
combined_50_h=ttest2(combined_50_cd,baseline_50_cd,'Alpha',.01,'Tail','left','Vartype','unequal')
;
boxfish_55_h=ttest2(boxfish_55_cd,baseline_55_cd,'Alpha',.01,'Tail','left','Vartype','unequal');
shark_55_h=ttest2(shark_55_cd,baseline_55_cd,'Alpha',.01,'Tail','left','Vartype','unequal');
combined_55_h=ttest2(combined_55_cd,baseline_55_cd,'Alpha',.01,'Tail','left','Vartype','unequal')
;
boxfish_60_h=ttest2(boxfish_60_cd,baseline_60_cd,'Alpha',.01,'Tail','left','Vartype','unequal');
shark_60_h=ttest2(shark_60_cd,baseline_60_cd,'Alpha',.01,'Tail','left','Vartype','unequal');
combined_60_h=ttest2(combined_60_cd,baseline_60_cd,'Alpha',.01,'Tail','left','Vartype','unequal')
;
```

```
boxfish_65_h=ttest2(boxfish_65_cd,baseline_65_cd,'Alpha',.01,'Tail','left','Vartype','unequal');
shark_65_h=ttest2(shark_65_cd,baseline_65_cd,'Alpha',.01,'Tail','left','Vartype','unequal');
combined_65_h=ttest2(combined_65_cd,baseline_65_cd,'Alpha',.01,'Tail','left','Vartype','unequal')
;
boxfish_70_h=ttest2(boxfish_70_cd,baseline_70_cd,'Alpha',.01,'Tail','left','Vartype','unequal');
shark_70_h=ttest2(shark_70_cd,baseline_70_cd,'Alpha',.01,'Tail','left','Vartype','unequal');
combined_70_h=ttest2(combined_70_cd,baseline_70_cd,'Alpha',.01,'Tail','left','Vartype','unequal')
;
boxfish_75_h=ttest2(boxfish_75_cd,baseline_75_cd,'Alpha',.01,'Tail','left','Vartype','unequal');
shark_75_h=ttest2(shark_75_cd,baseline_75_cd,'Alpha',.01,'Tail','left','Vartype','unequal');
combined_75_h=ttest2(combined_75_cd,baseline_75_cd,'Alpha',.01,'Tail','left','Vartype','unequal')
;
boxfish_80_h=ttest2(boxfish_80_cd,baseline_80_cd,'Alpha',.01,'Tail','left','Vartype','unequal');
shark_80_h=ttest2(shark_80_cd,baseline_80_cd,'Alpha',.01,'Tail','left','Vartype','unequal');
combined_80_h=ttest2(combined_80_cd,baseline_80_cd,'Alpha',.01,'Tail','left','Vartype','unequal')
;
boxfish_85_h=ttest2(boxfish_85_cd,baseline_85_cd,'Alpha',.01,'Tail','left','Vartype','unequal');
shark_85_h=ttest2(shark_85_cd,baseline_85_cd,'Alpha',.01,'Tail','left','Vartype','unequal');
combined_85_h=ttest2(combined_85_cd,baseline_85_cd,'Alpha',.01,'Tail','left','Vartype','unequal')
;
x={'40 mph' '45 mph' '50 mph' '55 mph' '60 mph' '65 mph' '70 mph' '75 mph' '80 mph' '85 mph'};
table2=string(zeros(30,1));
i=1;
if boxfish_40_h==1
    table2{i}='    Reject H0    ';
else
    table2{i}='Fail to Reject H0';
end
if shark_40_h==1
    table2{i+1}='    Reject H0    ';
else
    table2{i+1}='Fail to Reject H0';
end
if combined_40_h==1
    table2{i+2}='    Reject H0    ';
else
    table2{i+2}='Fail to Reject H0';
end
if boxfish_45_h==1
    table2{i+3}='    Reject H0    ';
else
    table2{i+3}='Fail to Reject H0';
end
if shark_45_h==1
    table2{i+4}='    Reject H0    ';
else
    table2{i+4}='Fail to Reject H0';
end
if combined_45_h==1
    table2{i+5}='    Reject H0    ';
else
    table2{i+5}='Fail to Reject H0';
end
i=i+6;
```

```
if boxfish_50_h==1
    table2{i}='    Reject H0    ';
else
    table2{i}='Fail to Reject H0';
end
if shark_50_h==1
    table2{i+1}='    Reject H0    ';
else
    table2{i+1}='Fail to Reject H0';
end
if combined_50_h==1
    table2{i+2}='    Reject H0    ';
else
    table2{i+2}='Fail to Reject H0';
end
if boxfish_55_h==1
    table2{i+3}='    Reject H0    ';
else
    table2{i+3}='Fail to Reject H0';
end
if shark_55_h==1
    table2{i+4}='    Reject H0    ';
else
    table2{i+4}='Fail to Reject H0';
end
if combined_55_h==1
    table2{i+5}='    Reject H0    ';
else
    table2{i+5}='Fail to Reject H0';
end
i=i+6;
if boxfish_60_h==1
    table2{i}='    Reject H0    ';
else
    table2{i}='Fail to Reject H0';
end
if shark_60_h==1
    table2{i+1}='    Reject H0    ';
else
    table2{i+1}='Fail to Reject H0';
end
if combined_60_h==1
    table2{i+2}='    Reject H0    ';
else
    table2{i+2}='Fail to Reject H0';
end
if boxfish_65_h==1
    table2{i+3}='    Reject H0    ';
else
    table2{i+3}='Fail to Reject H0';
end
if shark_65_h==1
    table2{i+4}='    Reject H0    ';
else
```

```
    table2{i+4}='Fail to Reject H0';
end
if combined_65_h==1
    table2{i+5}='    Reject H0    ';
else
    table2{i+5}='Fail to Reject H0';
end
i=i+6;
if boxfish_70_h==1
    table2{i}='    Reject H0    ';
else
    table2{i}='Fail to Reject H0';
end
if shark_70_h==1
    table2{i+1}='    Reject H0    ';
else
    table2{i+1}='Fail to Reject H0';
end
if combined_70_h==1
    table2{i+2}='    Reject H0    ';
else
    table2{i+2}='Fail to Reject H0';
end
if boxfish_75_h==1
    table2{i+3}='    Reject H0    ';
else
    table2{i+3}='Fail to Reject H0';
end
if shark_75_h==1
    table2{i+4}='    Reject H0    ';
else
    table2{i+4}='Fail to Reject H0';
end
if combined_75_h==1
    table2{i+5}='    Reject H0    ';
else
    table2{i+5}='Fail to Reject H0';
end
i=i+6;
if boxfish_80_h==1
    table2{i}='    Reject H0    ';
else
    table2{i}='Fail to Reject H0';
end
if shark_80_h==1
    table2{i+1}='    Reject H0    ';
else
    table2{i+1}='Fail to Reject H0';
end
if combined_80_h==1
    table2{i+2}='    Reject H0    ';
else
    table2{i+2}='Fail to Reject H0';
end
```

```
if boxfish_85_h==1
    table2{i+3}='    Reject H0    ';
else
    table2{i+3}='Fail to Reject H0';
end
if shark_85_h==1
    table2{i+4}='    Reject H0    ';
else
    table2{i+4}='Fail to Reject H0';
end
if combined_85_h==1
    table2{i+5}='    Reject H0    ';
else
    table2{i+5}='Fail to Reject H0';
end
i=i*0+1;
j=1;
fprintf('\nSTATISTICAL HYPOTHESIS TEST\nTwo-Sample t-Test at Significance Level = 0.01\n')
fprintf('Null Hypothesis, H0 = The drag coefficient of the bio-inspired design is equal to the
drag coefficient of the baseline design.\n')
fprintf('Alternative Hypothesis, H1 = The drag coefficient of the bio-inspired design is less
than the drag coefficient of the baseline design.\n')
fprintf('|--------|-------------------------------------------------------------|\n')
fprintf('|        |                    Bio-Inspired Design                      |\n')
fprintf('|        |-------------------|-------------------|-------------------|\n')
fprintf('|        |     Design 2      |     Design 3      |     Design 4      |\n')
fprintf('| Speed  |     (Boxfish)     |     (Shark)       |    (Combined)     |\n')
fprintf('|--------|-------------------|-------------------|-------------------|\n| %1$s | %2$s |
%3$s | %4$s |\n',x{j},table2{i},table2{i+1},table2{i+2})
i=i+3;
j=j+1;
fprintf('|--------|-------------------|-------------------|-------------------|\n| %1$s | %2$s |
%3$s | %4$s |\n',x{j},table2{i},table2{i+1},table2{i+2})
i=i+3;
j=j+1;
fprintf('|--------|-------------------|-------------------|-------------------|\n| %1$s | %2$s |
%3$s | %4$s |\n',x{j},table2{i},table2{i+1},table2{i+2})
i=i+3;
j=j+1;
fprintf('|--------|-------------------|-------------------|-------------------|\n| %1$s | %2$s |
%3$s | %4$s |\n',x{j},table2{i},table2{i+1},table2{i+2})
i=i+3;
j=j+1;
fprintf('|--------|-------------------|-------------------|-------------------|\n| %1$s | %2$s |
%3$s | %4$s |\n',x{j},table2{i},table2{i+1},table2{i+2})
i=i+3;
j=j+1;
fprintf('|--------|-------------------|-------------------|-------------------|\n| %1$s | %2$s |
%3$s | %4$s |\n',x{j},table2{i},table2{i+1},table2{i+2})
i=i+3;
j=j+1;
fprintf('|--------|-------------------|-------------------|-------------------|\n| %1$s | %2$s |
%3$s | %4$s |\n',x{j},table2{i},table2{i+1},table2{i+2})
i=i+3;
```

```
j=j+1;
fprintf('|--------|--------------------|--------------------|--------------------|\n| %1$s | %2$s |
%3$s | %4$s |\n',x{j},table2{i},table2{i+1},table2{i+2})
i=i+3;
j=j+1;
fprintf('|--------|--------------------|--------------------|--------------------|\n| %1$s | %2$s |
%3$s | %4$s |\n',x{j},table2{i},table2{i+1},table2{i+2})
i=i+3;
j=j+1;
fprintf('|--------|--------------------|--------------------|--------------------|\n| %1$s | %2$s |
%3$s | %4$s |\n',x{j},table2{i},table2{i+1},table2{i+2})
i=i+3;
j=j+1;
fprintf('|--------|--------------------|--------------------|--------------------|\n')
```

SUMMARY STATISTICS

	Design 1 (Baseline)			Design 2 (Boxfish)			Design 3 (Shark)			Design 4 (Combined)		
Speed	Cd	Stdev	N	Cd	Stdev	N	Cd	Stdev	N	Cd	Stdev	N
40 mph	0.45	0.023	2997	0.37	0.026	2997	0.39	0.022	2997	0.35	0.043	2997
45 mph	0.50	0.033	2997	0.42	0.024	2997	0.44	0.023	2997	0.39	0.026	2997
50 mph	0.53	0.026	2997	0.46	0.024	2997	0.48	0.020	2997	0.43	0.019	2997
55 mph	0.55	0.019	2997	0.49	0.020	2997	0.51	0.017	2997	0.46	0.019	2997
60 mph	0.57	0.017	2997	0.51	0.020	2997	0.54	0.016	2997	0.49	0.019	2997
65 mph	0.59	0.018	2997	0.53	0.021	2997	0.56	0.017	2997	0.51	0.020	2997
70 mph	0.60	0.017	2997	0.54	0.020	2997	0.57	0.017	2997	0.52	0.017	2997
75 mph	0.61	0.015	2997	0.56	0.017	2997	0.58	0.016	2997	0.53	0.018	2997
80 mph	0.62	0.016	2997	0.56	0.017	2997	0.59	0.014	2997	0.54	0.017	2997
85 mph	0.62	0.016	2997	0.56	0.016	2997	0.59	0.013	2997	0.54	0.015	2997

STATISTICAL HYPOTHESIS TEST

Two-Sample t-Test at Significance Level = 0.01

Null Hypothesis, H0 = The drag coefficient of the bio-inspired design is equal to the drag coefficient of the baseline design.

Alternative Hypothesis, H1 = The drag coefficient of the bio-inspired design is less than the drag coefficient of the baseline design.

	Bio-Inspired Design		
Speed	Design 2 (Boxfish)	Design 3 (Shark)	Design 4 (Combined)
40 mph	Reject H0	Reject H0	Reject H0
45 mph	Reject H0	Reject H0	Reject H0
50 mph	Reject H0	Reject H0	Reject H0
55 mph	Reject H0	Reject H0	Reject H0
60 mph	Reject H0	Reject H0	Reject H0
65 mph	Reject H0	Reject H0	Reject H0
70 mph	Reject H0	Reject H0	Reject H0
75 mph	Reject H0	Reject H0	Reject H0
80 mph	Reject H0	Reject H0	Reject H0
85 mph	Reject H0	Reject H0	Reject H0

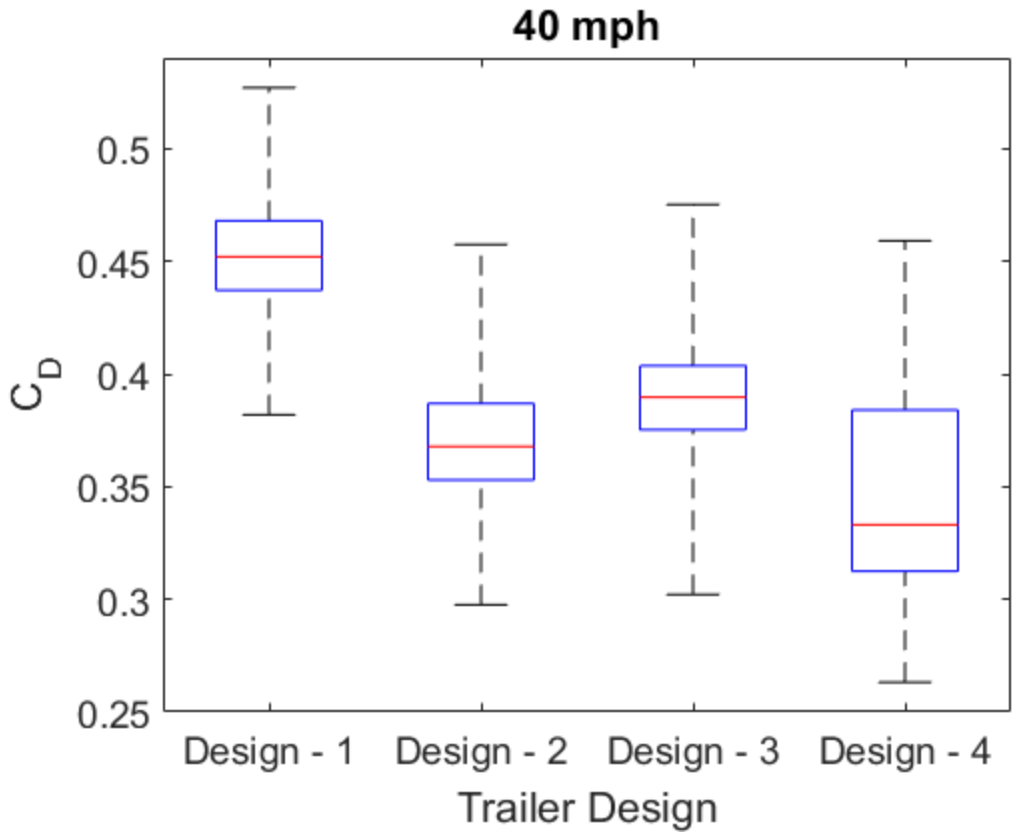
40 mph
0.5
0.45
0.4
0.35
0.3
0.25
C_D
Design - 1
Design - 2
Design - 3
Design - 4
Trailer Design

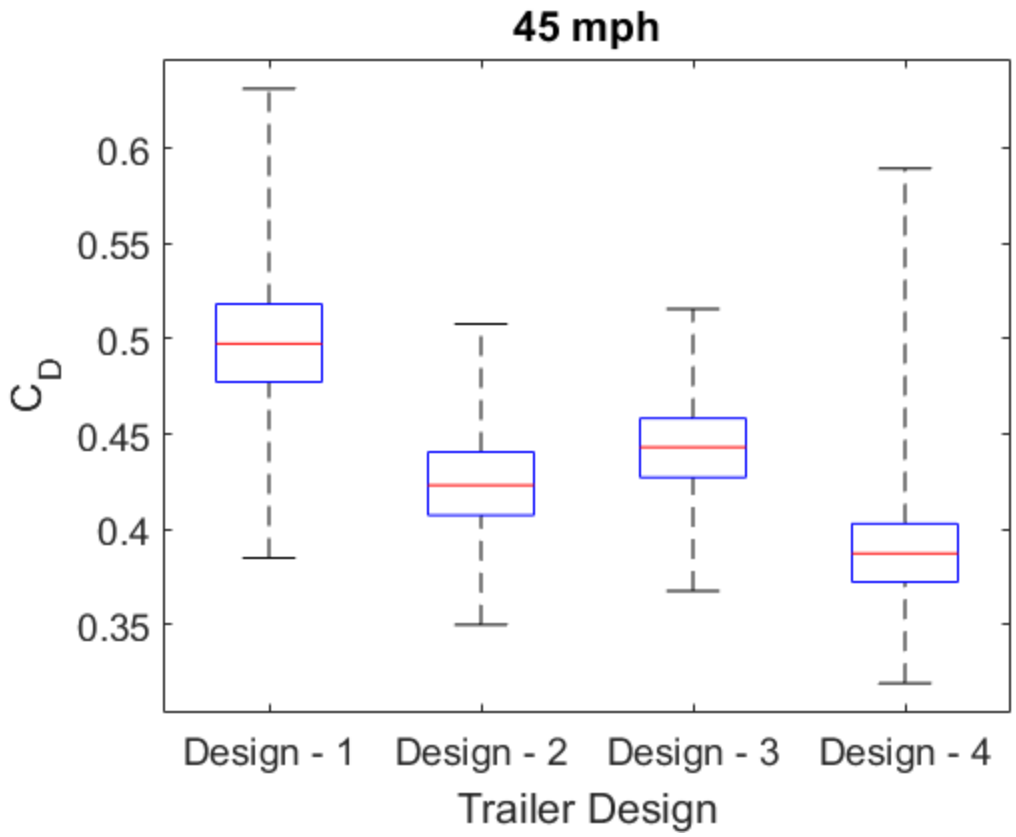
45 mph
0.6
0.55
0.5
0.45
0.4
0.35
C_D
Design - 1
Design - 2
Design - 3
Design - 4
Trailer Design

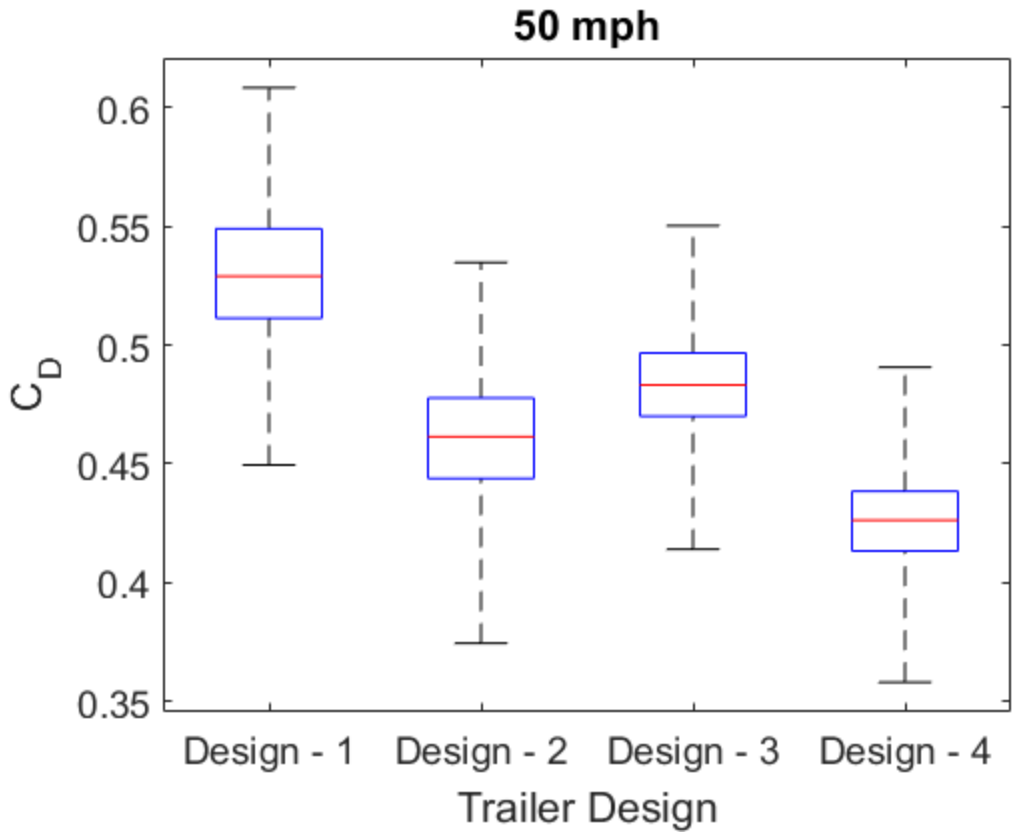
50 mph
0.6
0.55
0.5
0.45
0.4
0.35
C_D
Design - 1
Design - 2
Design - 3
Design - 4
Trailer Design

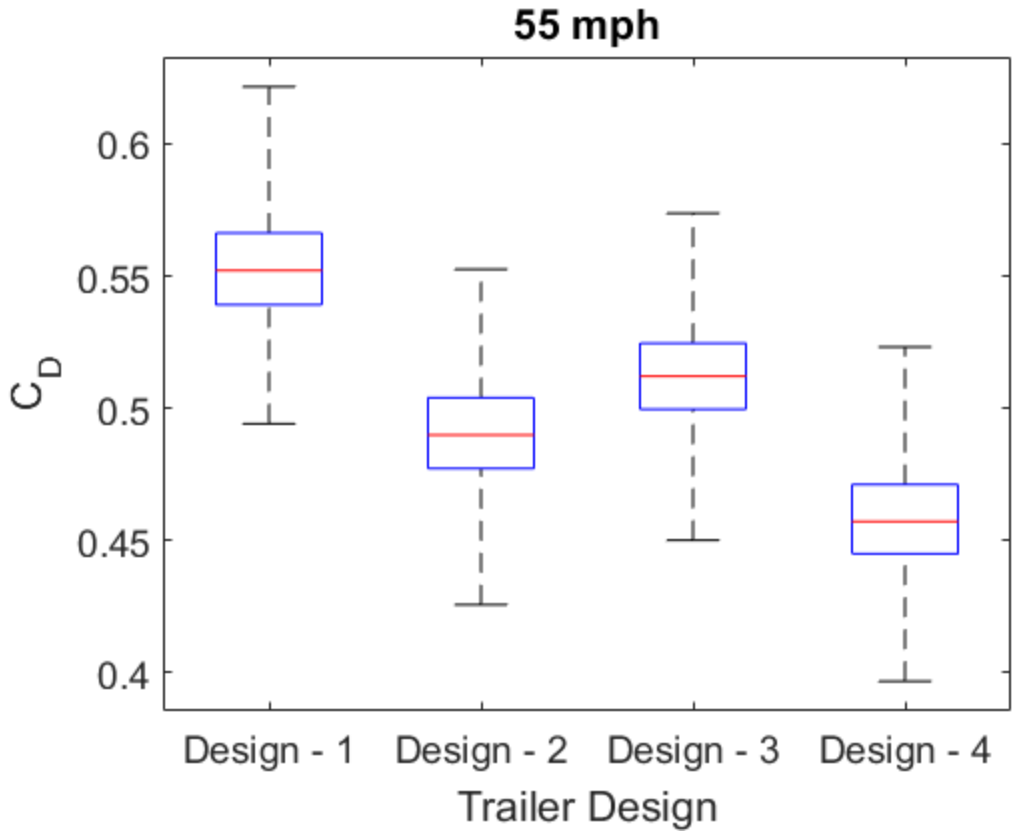
55 mph
0.6
0.55
0.5
0.45
0.4
C_D
Design - 1
Design - 2
Design - 3
Design - 4
Trailer Design

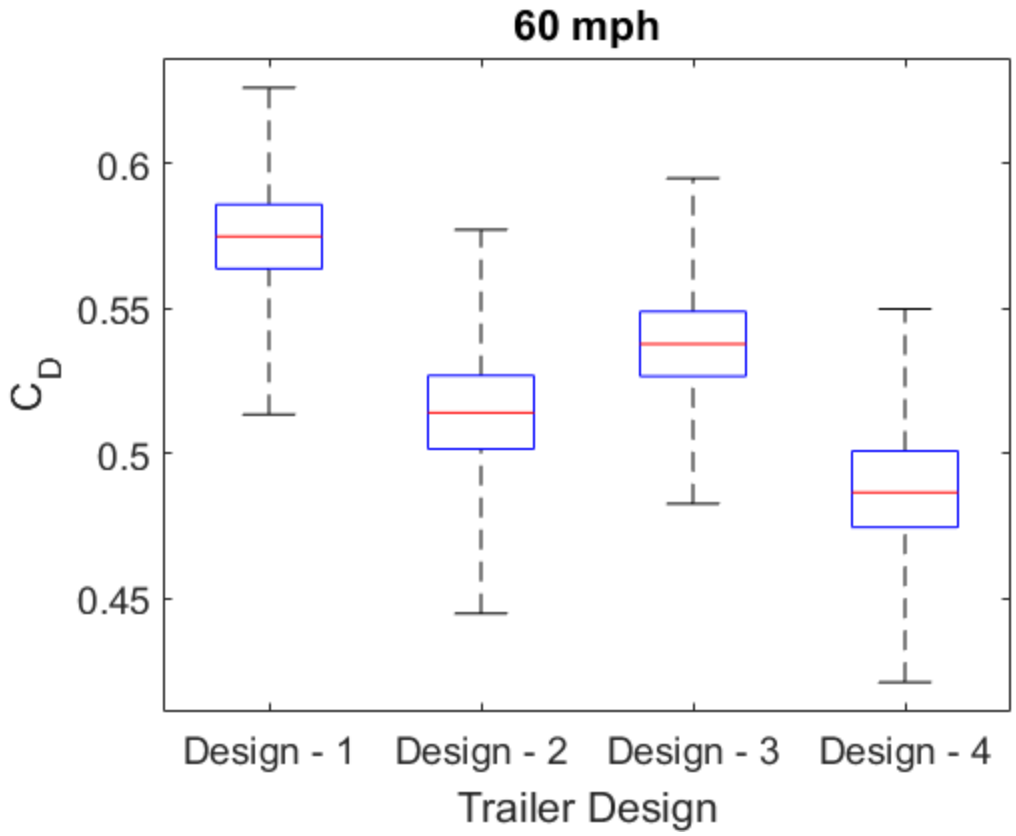
60 mph
0.6
0.55
0.5
0.45
C_D
Design - 1
Design - 2
Design - 3
Design - 4
Trailer Design

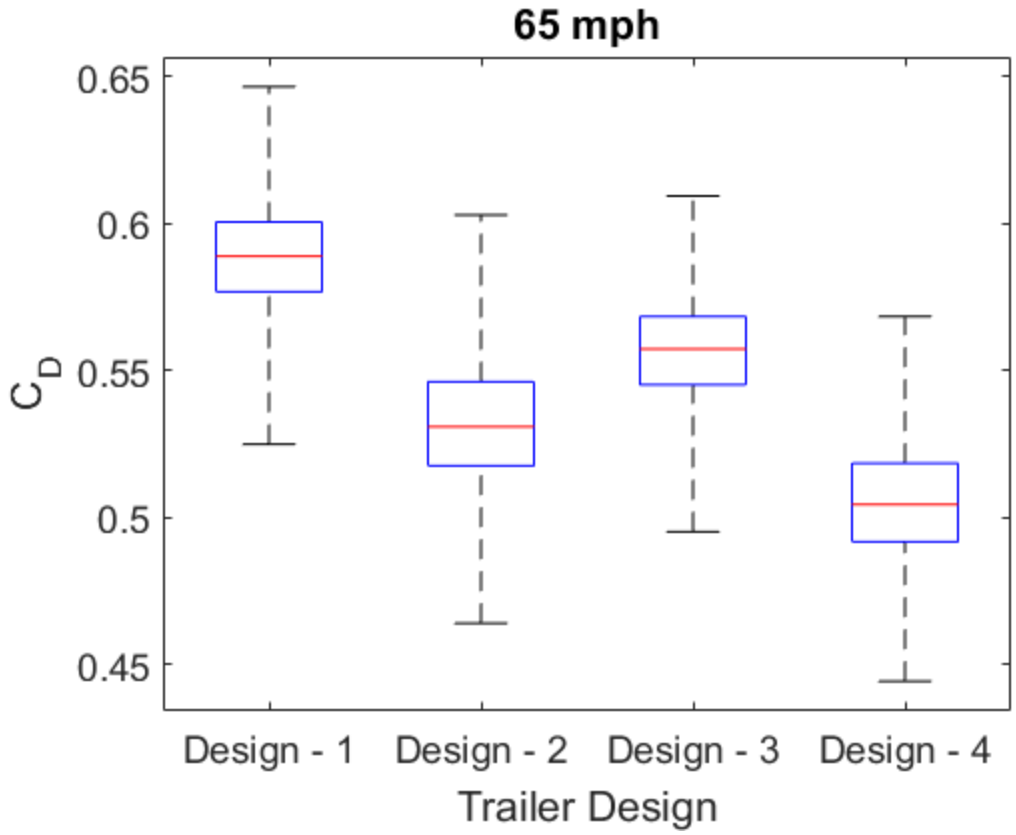
65 mph
0.65
0.6
0.55
0.5
0.45
C_D
Design - 1
Design - 2
Design - 3
Design - 4
Trailer Design

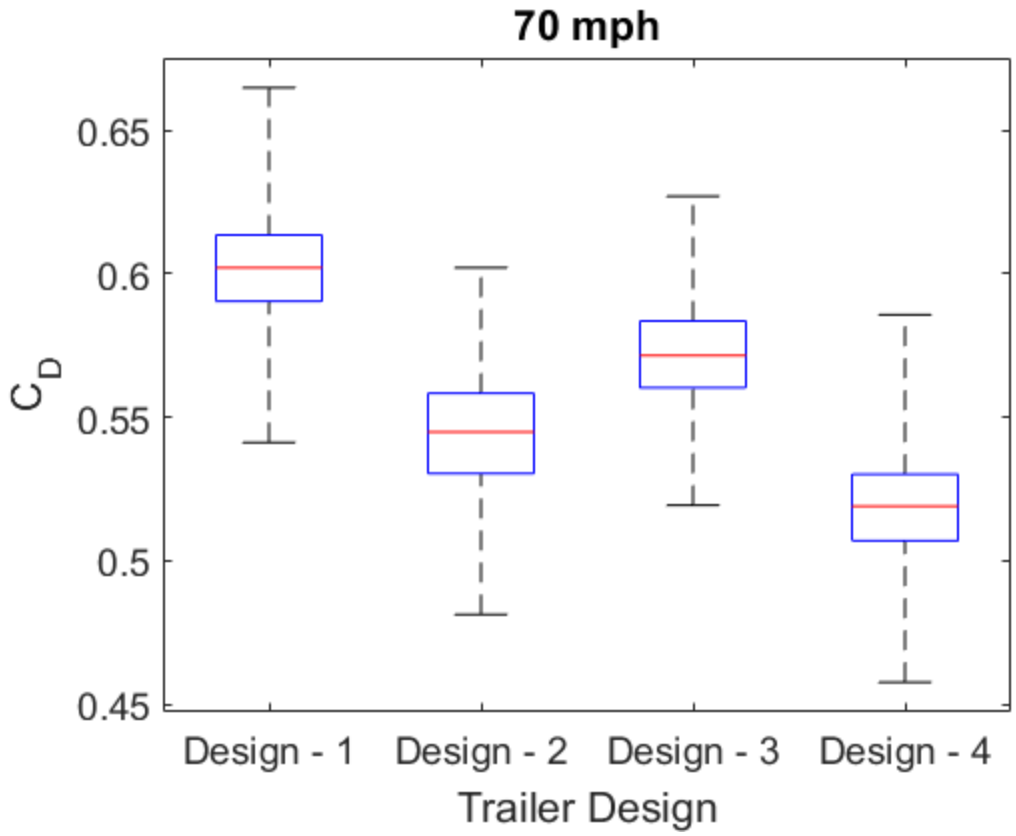
70 mph
0.65
0.6
0.55
0.5
0.45
C_D
Design - 1
Design - 2
Design - 3
Design - 4
Trailer Design

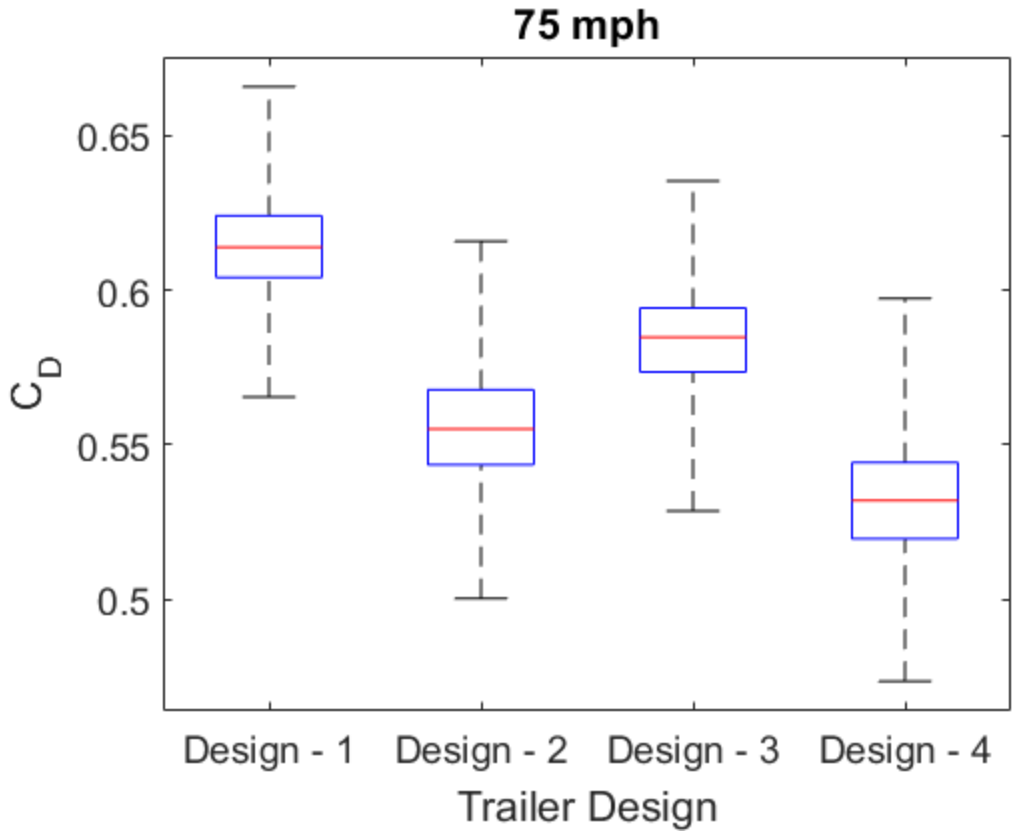
75 mph
0.65
0.6
0.55
0.5
C_D
Design - 1
Design - 2
Design - 3
Design - 4
Trailer Design

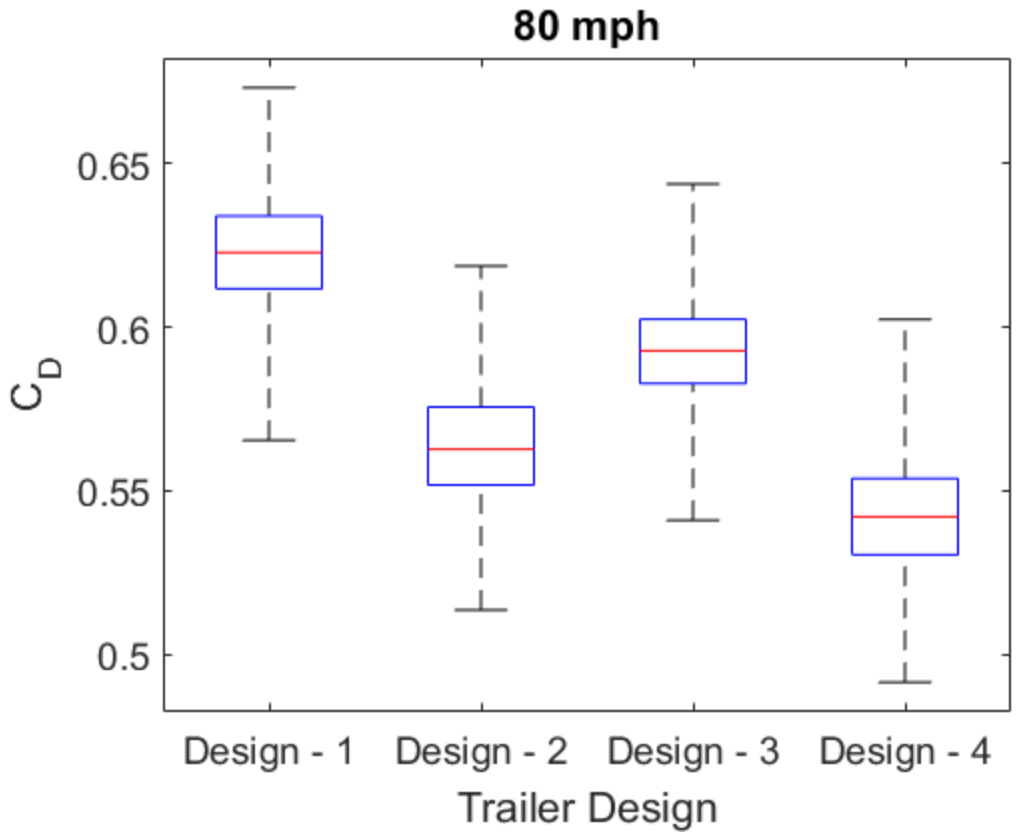
80 mph
0.65
0.6
0.55
0.5
C_D
Design - 1
Design - 2
Design - 3
Design - 4
Trailer Design

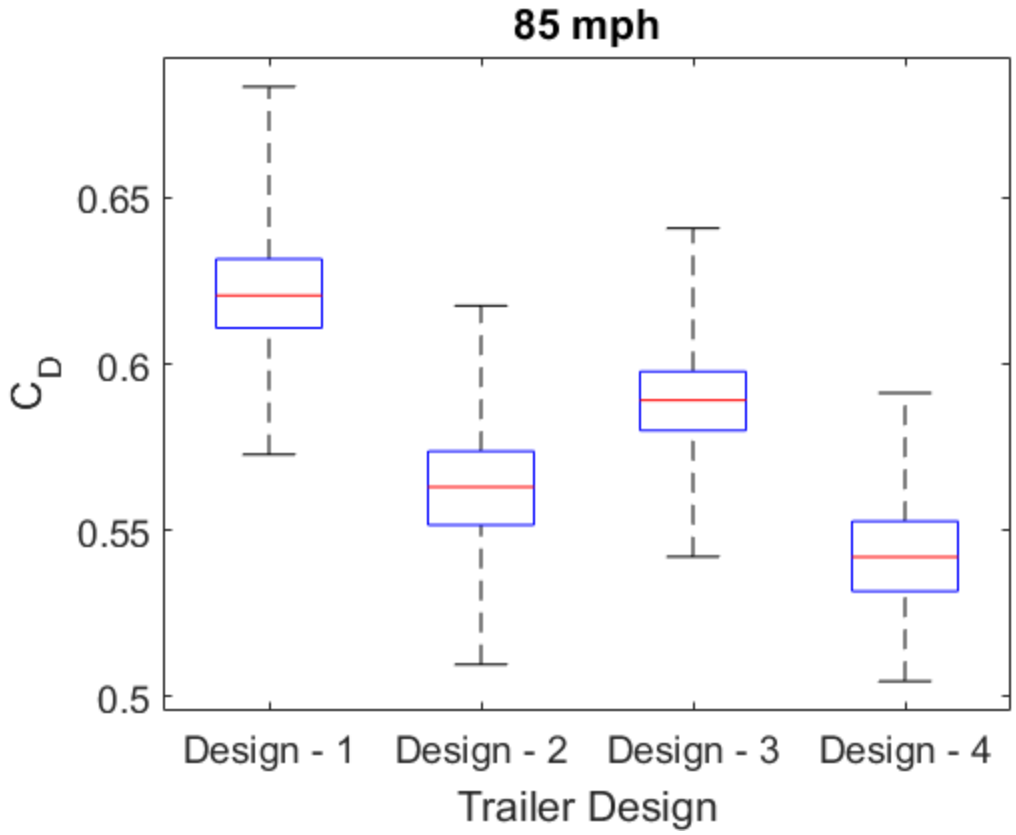
85 mph
0.65
0.6
0.55
0.5
C_D
Design - 1
Design - 2
Design - 3
Design - 4
Trailer Design

REFERENCES

[1] Bureau of Transportation Statistics, "Freight Facts and Figures," U.S. Department of Transportation, 2015.

[2] Office of Transportation and Air Quality, "Fuel Economy," U.S. Department of Energy, [Online]. Available: https://www.fueleconomy.gov/feg/Find.do?action=sbs&id=38429.

[3] G. Di Lullo, H. Zhang and A. Kumar, "Evaluation of uncertainty in the well-to-tank and combustion greenhouse gas emissions of various transpotation fuels," *Applied Energy,* vol. 184, pp. 413-426, 2016.

[4] A. M. Williamson, O. Badr and S. D. Probert, "Reliance of British transport on fossil fuels: Associated adverse impacts on air quality," *Applied Energy,* vol. 56, pp. 27-45, 1997.

[5] Y. Zeng, X. Tan, B. Gu, Y. Wang and B. Xu, "Greenhouse gas emissions of motor vehicles in Chinese cities and the implication for China's mitigation targets," *Applied Energy,* vol. 184, pp. 1016-1025, 2016.

[6] M. Su, S. Pauleit, X. Yin, Y. Zheng, S. Chen and C. Xu, "Greenhouse gas emissions accounting for EU member states from 1991 to 2012," *Applied Energy,* vol. 184, pp. 759-768, 2016.

[7] J. Woodcock, P. Edwards, C. Tonne, B. G. Armstrong, O. Ashiru, D. Banister and e. al., "Public health benefits of strategies to reduce greenhouse-gas emissions: urban land transport," *The Lancet,* vol. 374, no. 9705, pp. 1930-1943, 2009.

[8] R. Bradley, "Technology Roadmap for the 21st Century Truck Program," U.S.

Department of Energy, 2000.

[9] K. R. Cooper, "The Effect of Front-Edge Rounding and Rear-Edge Shaping on the Aerodynamic Drag of Bluff Vehicles in Ground Proximity," *SAE Technical Paper 850288,* 1985.

[10] H. Martini, B. Bergqvist, L. Hjelm and L. Lofdahl, "Influence of Different Truck and Trailer Combinations on the Aerodynamic Drag," *SAE International,* 2011.

[11] H. Choi, J. Lee and H. Park, "Aerodynamics of Heavy Vehicles," *Annual Review of Fluid Mechanics,* vol. 46, pp. 441-468, 2014.

[12] K. R. Cooper, "Truck Aerodynamics Reborn - Lessons from the Past," in *SAE International Truck and Bus Meeting and Exhibition*, Fort Worth, 2003.

[13] "Prostar ES," International Trucks, [Online]. Available: https://www.internationaltrucks.com/prostar-es. [Accessed 8 March 2017].

[14] "TrailerTail® Fuel Savings Technology," STEMCO, [Online]. Available: http://www.stemco.com/product/trailertail/. [Accessed 9 March 2017].

[15] D. Friedman, "SuperTruck Leading the Way for Efficiency in Heavy-Duty, Long-Haul Vehicles," Office of Energy Efficiency and Renewable Energy, 27 June 2016. [Online]. Available: https://energy.gov/eere/articles/supertruck-leading-way-efficiency-heavy-duty-long-haul-vehicles. [Accessed 7 March 2017].

[16] "CUMMINS-PETERBILT SUPERTRUCK ACHIEVES 10.7 MPG IN LATEST TEST," Peterbilt, 18 February 2014. [Online]. Available: http://www.peterbilt.com/about/media/2014/396/. [Accessed 9 March 2017].

[17] "The SuperTruck Challenge," Daimler, [Online]. Available: http://www.freightlinersupertruck.com/#main. [Accessed 9 March 2017].

[18] "NAVISTAR'S SUPERTRUCK EXCEEDS DEPARTMENT OF ENERGY'S FREIGHT EFFICIENCY GOAL," Navistar, 28 September 2016. [Online]. Available: http://media.navistar.com/index.php?s=43&item=812. [Accessed 9 March 2017].

[19] "SuperTruck," Volvo, 2016. [Online]. Available: http://www.volvotrucks.us/about-volvo/supertruck/. [Accessed 9 March 2017].

[20] J. S. Reiskin, "Navistar Demos Platooning Technology, Concept Vehicle With New LT, HX Series Trucks," Transport Topics, 14 October 2016. [Online]. Available: http://www.ttnews.com/articles/basetemplate.aspx?storyid=43538. [Accessed 9 March 2017].

[21] M. Mueller, "Video: Volvo SuperTruck Visits Energy Department," U.S. Department of Energy, 15 September 2016. [Online]. Available: https://energy.gov/sites/prod/files/SuperTruck_Front%20angle_wide.png. [Accessed 9 Mach 2017].

[22] B. Bhushan, "Biomimetics: lessons from nature-an overview," *Philosophical Transactions of the Royal Society A,* vol. 367, no. 1893, pp. 1445-1486, 2009.

[23] K. Bartol, M. S. Gordon, P. Webb, D. Weihs and M. Gharib, "Evidence of self-correcting spiral flows in swimming boxfishes," *Bioinspiration & Biomimetics,* vol. 3, no. 1, 2008.

[24] F. G. Carey and J. M. Teal, "Mako and Porbeagle: Warm-bodied Sharks," *Comparative Biochemistry and Physiology,* vol. 28, no. 1, pp. 199-204, 1969.

[25] B. R. Munson, T. H. Okiishi, W. W. Huebsch and A. P. Rothmayer, Fundamentals of

Fluid Mechanics, Hoboken: John Wiley & Sons, Inc., 2013.

[26] H. L. J. Pratt and J. G. Casey, "Age and Growth of the Shortfin Mako, Isurus oxyrinchus, Using Four Methods," *Canadian Journal of Fisheries and Aquatic Sciences,* vol. 40, no. 11, pp. 1944-1957, 1983.

[27] J. H. Bell and R. D. Mehta, "Contraction Design for Small Low-Speed Wind Tunnels," Joint Institute for Aerodynamics and Acoustics, 1988.

[28] "FC22 Compression Load Cell," 2015. [Online]. Available: http://www.te.com/commerce/DocumentDelivery/DDEController?Action=showdoc&DocId=Data+Sheet%7FFC22%7FA%7Fpdf%7FEnglish%7FENG_DS_FC22_A.pdf%7FCAT-FSE0001. [Accessed 24 March 2017].

[29] "TruStability® Board Mount Pressure Sensors," August 2014. [Online]. Available: https://sensing.honeywell.com/honeywell-sensing-trustability-hsc-series-high-accuracy-board-mount-pressure-sensors-50099148-a-en.pdf. [Accessed 24 March 2017].

[30] S. R. Ahmed, R. G. Gawthorpe and P. -A. Mackrodt, "Aerodynamics of Road- and Rail Vehicles," *International Journal of Vehicle Mechanics and Mobility,* vol. 14, no. 4-6, pp. 319-392, 1985.